PHEOCHROMOCYTOMA-INDUCED CARDIOMYOPATHY: A MODEL OF SYNERGISTIC EFFECTS OF MULTIFACTORIAL TUMOR SECRETIONS

BY

HECTOR R. MOBINE
B.S. BIOENGINEERING, 2004
M.ENG. BIOENGINEERING, 2005
UNIVERSITY OF CALIFORNIA, SAN DIEGO

SUBMITTED TO THE DEPARTMENT OF BIOLOGICAL ENGINEERING
IN PARTIAL FULFILLMENT OF THE REQUIREMENTS FOR THE DEGREE OF

DOCTOR OF PHILOSOPHY IN BIOLOGICAL ENGINEERING
AT THE
MASSACHUSETTS INSTITUTE OF TECHNOLOGY
DECEMBER 2008
[February 2009]

SCIENCE

SIGNATURE OF AUTHOR:____
DEPARTMENT OF BIOLOGICAL ENGINEERING

CERTIFIED BY: _____
ELAZER R. EDELMAN
THOMAS D. AND VIRGINIA W. CABOT PROFESSOR OF
HEALTH SCIENCES & TECHNOLOGY
ADVISOR

CERTIFIED BY: _____
ROB ERT LANGER
GERMESHAUSEN PROFESSOR OF CHEMICAL AND BIOMEDICAL ENGINEERING
CO-ADVISOR

CERTIFIED BY: _____
ALAN J. GRODZINSKY
PROFESSOR OF ELECTRICAL MECHANICAL, & BIOLOGICAL ENGINEERING
CHAIR, COURSE XX GRADUATE PROGRAM COMMITTEE

This doctoral thesis has been examined and approved by a committee of the Department of Biological Engineering as follows:

Professor Elazer Edelman _____

Professor John Essigmann _____

Professor Robert Langer _____

Professor Ram Sasisekharan _____

Professor Jonathan Seidman _____

PHEOCHROMOCYTOMA-INDUCED CARDIOMYOPATHY: A MODEL OF SYNERGISTIC EFFECTS OF MULTIFACTORIAL TUMOR SECRETIONS

Hector R. Mobine

Abstract

One specific thesis of pathogenesis holds that diseases are dependent upon the complex interactions of multiple compounds and cofactors. While one agent may dominate, its powerful effects are mediated by ancillary factors that alone may have no discernible action. We examined this paradigm by comparing catecholamine-infusion induced cardiomyopathy with the organ disease observed by catecholamine-secreting pheochromocytoma cells.

Pheochromocytomas are widely believed to induce cardiomyopathy via hypersecretion of catecholamines including norepinephrine (NE). NE can have direct cardiomyocyte toxicity and can stimulate myocardial remodeling secondary to the induction of hypertension. Yet, cardiomyopathy development is not entirely related to catecholamine dose. To explore these effects we engineered a polymeric cell encapsulation system to control PC12 cell kinetics and NE release *in vitro* and *in vivo.* We demonstrated that pheochromocytoma-conditioned media induced greater cardiomyocyte contractility and cytoskeletal remodeling than NE alone. We next examined the cardiomyopathy development in animals implanted with agarose-encapsulated pheochromocytoma (PC12) cells, DOPA decarboxylase knock-out PC12

cells deficient in norepinephrine (PC12-KO), or norepinephrine-secreting pumps. Implanted PC12 cells induced a greater degree of cardiomyopathy than animals dosed only with norepinephrine. Elimination of norepinephrine secretion in PC12-KO cells eliminated the effects of PC12 cells, while reintroduction of NE secretion via NE secreting pumps implanted alongside PC12-KO cells induced a cardiac pathology similar to intact PC12 cells.

In the second portion of this work, we examined the role of pregnancy in our disease model and its ability to exacerbate pheochromocytoma-induced cardiomyopathy. Gravid pheochromocytoma-bearing mice experienced a greater loss of cardiac function and increased expansion of cardiac volume compared to non-gravid pheochromocytoma-bearing mice. Our data suggest that it is the confluence of these factors that enable the synergistic induction of myocardial injury. The implications of our work lie not only in a better understanding of pheochromocytomas and their secretory products but also in the differences between cell-secreted substances and their exogenous analogues in isolation.

Thesis committee: Professor Ram Sasisekharan, Committee Chairman

Professor Elazer Edelman, Advisor

Professor Robert Langer, Co-Advisor

Professor John Essigmann

Professor Jon Seidman

ACKNOWLEDGMENTS

This thesis would not be possible (nor very useful) without the guidance, patience, and support of various people.

Professor Elazer Edelman played an integral role in this work, and more importantly in my development as a scientist. He took a risk in me and allowed me the freedom to pursue my ideas. Regardless of his schedule he always made time to discuss my issues, however large or small. I will always be indebted to him for all he has taught me. Professor Jonathan Seidman's time and resources were essential to the successful completion of this work as well. His insight and advice were always sought out and extremely helpful. Professor's John Essigmann, Ram Sasisekharan, and Robert Langer served on my thesis committee. Their critical review of my work was a tremendous help.

I owe a great deal to my colleagues, whose hard work and guidance were integral to the success of my work. Dr. Aaron Baker was a wonderful collaborator, he was a sounding board to my ideas and his hard work was instrumental to my first publication. Drs. Libin Wang and Hiroko Wakimoto devoted a great deal of time and effort in performing echocardiograms. I also am grateful to the patience and insight given by Dr. James Stanley, Gee Wong, and Phil Seifert. Tarek Elshazly was a great friend, a wonderful distraction to the long days in lab and an always-willing troubleshooter. He is a wonderful scientist and a great friend.

I would especially like to thank my family. Their unwavering support and understanding have played an integral role in my success.

TABLE OF CONTENTS

1 List of Figures

2 List of Tables

3 Introduction

3.1 Pheochromocytomas

Pheochromocytomas are rare catecholamine-producing neuroendocrine tumors that arise from chromaffin cells of the adrenal medulla or extra-adrenal paraganglia. Pheochromocytomas affect more women than men, usually occurring in adults between 30-40 years of age(1). Pheochromocytomas, regarded as the "10%" tumor, are malignant in 10% of cases, 10% bilateral pheochromocytomas, and 10% of cases are believed to be hereditary (2-4). The clinical presentation of pheochromocytomas is highly variable. Most, but not all, of the clinical signs and symptoms of pheochromocytomas arise from the direct actions of secreted catecholamines, epinephrine and norepinephrine (NE). Hypertension, tachycardia, excessive sweating, pallor, headache, and feelings of panic or anxiety usually describe the clinical presentation. Metabolic effects include hyperglycemia, lactic acidosis, and weight loss. In short, most of these signs and symptoms are reflective of a hyperadrenergic state associated with excessive catecholamine drive. Left undetected and untreated, end organ effects such as hypertensive heart disease and subsequently dilated cardiomyopathy ensue.

3.1.1 Etiology

Pheochromocytomas are benign tumors of the chromaffin cells of the adrenal medulla, which are benign in 90% of cases. About 10% of patients with pheochromocytomas present with metastatic disease at the time of initial workup. As

many as 25% of patients with apparent sporadic pheochromocytomas, in absence of family history of the disease, may be carriers of germline mutations predisposing them to the development of neurofibromatosis 1, von Hippel-Lindau, multiple endocrine neoplasia type 1 and 2, and the pheochromocytoma/paraganglioma syndromes(5). Mutations in the succinate dehydrogenase (SDH) gene family, SDHB, SDHC, and SDHD, have been linked to the incidence of paragangliomas and pheochromocytomas(6-10).

3.2 Pheochromocytoma-Associated Cardiomyopathy

3.2.1 Treatment

The definitive treatment is surgical removal of the primary tumor. Without treatment the 5-year survival rate falls below 50%(11). Prior to surgical resection, therapy is concentrated on controlling the effects of the catecholamines via α- and β-adrenergic blockade. The preoperative use of α- and β-blockers has traditionally been advocated to counteract the sudden release of large quantities of catecholamines during surgical resections(12, 13). Calcium channel agonists are also used to control blood pressure and related symptoms by inhibiting NE-mediated release of intracellular calcium. This causes the arteriolar smooth muscle to relax and peripheral vascular resistance to decrease(14-16).

3.2.2 Models/Research

Several *in vivo* models have been established to investigate pheochromocytomas. The first experimental pheochromocytoma model was based on the development of a transplantable pheochromocytoma cell line that predominately secreted norepinephrine(17-20). The implanted pheochromocytoma cells grow rapidly and unbridled, increasing plasma NE concentrations 40- to 75-fold(18, 21). By 30 days the rats exhibited signs of catecholamine excess including hypertension and ß-adrenergic receptor desensitization(22, 23), rarely surviving beyond 60 days. These studies introduced evidence of alpha-adrenergic receptor (αAR) down-regulation without changes in receptor affinity(19) and ß-adrenergic receptor down-regulation with a reduced binding affinity for the remaining receptors(24). In addition, cardiac muscle retained a normal, and occasionally enhanced, response to exogenously administered calcium, despite histological damage(24). Cardiomyopathy diagnosis was based on increased heart weight and the presence of multifocal cardiac lesions, enhanced interstitial and replacement fibrosis, contraction band necrosis, and mixed inflammatory infiltrates(18, 19, 25). These initial models provided important evidence that pheochromocytoma-induced cardiomyopathy was not caused by the resulting hypertension(26). Similarly prolonged catecholamine administration has been shown to induce cardiomyopathy by the presence of multifocal lesion-containing mixed inflammatory infiltrates and acute myocyte degeneration. The nonspecific vasodilators hydrazine normalized systolic blood pressure but did not affect the severity of cardiomyopathy. Pharmacologic antagonism of either βAR with timolol or αAR with phentolamine or phenoxybenzamine moderately decreased blood pressure and reduced cardiotoxicity. However, the β antagonist produced greater effects than the

α antagonist. Cardiomyopathy has been experimentally induced by exogenously administered epinephrine(27, 28), reserpine, and norepinephrine(29, 30), producing histological markers indicative of cardiomyopathy.

Pheochromocytoma models also exist in transgenic and knock-out models, including neurofibromatosis mice and MEN 2B transgenics(31). Moreover, disruptions of a mouse tumor suppressor gene, tension homologue deleted on chromosome 10 (PTEN), as well as the gene for phosphatase, increase the incidence of pheochromocytomas(32, 33).

The histological markers found in these rat hearts share similarities to hearts subjected to large bolus injections of catecholamines including multifocal lesions, acute damage with cytoplasm granularity, and contraction band necrosis. The histological similarities coupled with the known cardiotoxic effects of catecholamines and the association of hypertension with cardiomyopathy led to the current conclusion that pheochromocytoma-induced cardiomyopathy (PICM) is only mediated by the tumoral hypersecretion of catecholamines. In parallel to their conclusions, the researchers introduced the possibility that more complex factors may exist. These factors may act in synergy with catecholamines and could be involved in the maintenance of hypertension, therefore playing a role in cardiomyopathy development(18, 34).

Early models of catecholamine-induced cardiomyopathy involved large bolus doses of catecholamines(35, 36) that poorly replicate the prolonged pharmacological effects of constantly elevated levels. The direct interaction of catecholamines with

cardiomyocytes has been well established to be toxic(37), introducing the possibility that the histological damage resulted from the direct interaction of catecholamines and cardiomyocytes. More recently prolonged catecholamine administration has been shown to induce cardiomyopathy by the presence of multifocal lesion-containing mixed inflammatory infiltrates and acute myocyte degeneration. Cardiomyopathy has been experimentally induced by exogenously administered epinephrine(27, 28), norepinephrine(29, 30), and methoxamine, producing histological markers indicative of cardiomyopathy. Although the histological lesions found in catecholamine-induced cardiomyopathy rats' hearts are similar to those found in rats harboring pheochromocytoma cells, the cardiac morphology and function may be different.

Several observations have been made relating the myocardial damage found in patients diagnosed with pheochromocytomas to that of patients treated with norepinephrine(36, 38). A further resemblance of the two diseases involves the cardiac functional improvement seen in patients whose pheochromocytoma has been excised and those in which catecholamine levels have been reduced to normal. Since it is believed that the major myocardial damage induced by the pheochromocytoma occurs due to its excessive release of catecholamine, an association can be drawn about the mode of damage induced by catecholamine overload. Studies involving catecholamine induced cardiomyopathy have demonstrated that an excess of catecholamines down-regulated β receptors while causing severe damage to myofibrils resulting in a global reduction of myocardial pump function. Further myocardial damage has been attributed to changes in the permeability of the sarcolemmal membrane resulting from excess norepinephrine. The increased membrane permeability allows for increased intracellular

calcium concentration, which is toxic to cells, giving rise to cellular necrosis. It has also been posited that the oxidized products of catecholamines may be toxic, causing further cell damage(39).

A review of recent clinical studies and data suggests that cardiomyopathy in the presence of pheochromocytomas is more than solely catecholamine-induced. Instead, a complex of factors secreted by pheochromocytoma cells may modulate the development of cardiomyopathy(40-45). Of note, up to 36% of patients with pheochromocytomas who develop PICM exhibit no hypertension or abnormal catecholamine levels(46).

The scarcity of pheochromocytoma models can be attributed in part to the lack of an established human cell line. In lieu of a human immortalized line, research has focused on the currently available cell lines from pheochromocytomas in rodents. These include rat pheochromocytoma (PC12) cells(47) and the more recently established mouse (MPC) cells(48). PC12 cells, developed from a tumor in New England Deaconess rats, are representative of a single cell in a tumor. MPC cells, in contrast, were developed from neurofibromatosis knock-out mice and exist in several variations with varying characteristics. PC12 cells, derived from a rat adrenal tumor, are morphologically and cytochemically similar to both human pheochromocytoma cells and their normal counterparts (47), exhibiting similar catecholamine synthesis, storage, and secretion. These cells differ from normal pheochromocytoma cells in their low or non-existent expression of phenylethanolamine-N-methyltransferase, the enzyme responsible for converting norepinephrine to epinephrine(49). Alternatively, MPC cell

express the enzyme phenylethanolamine-N-methyltransferase, thereby secreting both epinephrine and norepinephrine(42).

3.3 Pheochromocytoma-Associated Peripartum Cardiomyopathy

3.3.1 Current Knowledge

PPCM is relatively rare, affecting 1 in 40,000 gravid females with a peak in incidence during the 3rd trimester(50, 51). Left ventricular systolic dysfunction often presents as dilated cardiomyopathy. According to the *Peripartum Cardiomyopathy: National Heart, Lung and Blood Institute and Office of Rare Disease Workshop,* one of the determining characteristics of peripartum cardiomyopathy is "the absence of a determinable cause for cardiomyopathy," further indicating the lack of knowledge about the onset of cardiomyopathy and its progression toward congestive heart failure. Peripartum cardiomyopathy (PPCM) is not an idiopathic dilated cardiomyopathy that occurs during the peripartum period, nor is it an exacerbated state of a pre-existing dilated cardiomyopathy.

Several hypotheses about the onset of PPCM exist. Initially, it was suggested that PPCM resulted from poor nutrition, but subsequent studies found a large proportion of women with PPCM to have adequate nutritional status (52). Another hypothesis for the etiology of PPCM is viral myocarditis or an aberrant immune response to pregnancy (53). Viral damage to heart cells can initiate an autoimmune response to cardiac proteins. In response to the viral infection, cytokines, specifically IL-1, TNF-α, and interferon-γ, are up-regulated resulting in the recruitment of T cells. T cells can clear viral damage but may exacerbate cardiomyocyte damage. As a result, PPCM can be

self-contained and even subclinical, or rampant and permanently devastating. Autoimmune processes may play a role as well (54). In this hypothesis, the destruction of myocardial cells is a byproduct of the activation of the immune system through the recognition of fetal cells that have crossed the placenta wall. Patients with PPCM have shown elevated antibodies to mitochondrial adenine nucleotide translocator, branched chain α ketoacid dehydrogenase, and myosin, supporting the autoimmune hypothesis(53).

It cannot be overlooked that prior to the development of a pheochromocytoma, the release of catecholamines may already be elevated due to the stresses inherent in pregnancy(55). During the period of gestation, maternal epinephrine and norepinephrine levels remain fairly constant until the onset of labor, at which time all hormone levels markedly increase(56). The rise in catecholamine concentration is significant enough to cause cardiomyocyte damage. This damage in combination with high levels of catecholamines secreted by a pheochromocytoma can increase the proclivity for cardiomyopathy(39). Although pheochromocytomas are known to cause cardiomyopathy in men, the specific circumstances, specifically the increased levels of catecholamines during labor, may explain the large number of female patients that develop cardiomyopathy during their 5 month post-partum period(57). The increase in catecholamine levels in non-gravid and gravid females are summarized in Table 1.

Table 1. Catecholamine Levels: (URL = Upper Range Limit).

Strain	Pheochromocytoma	Gravid	[NE] pg/ml	[EPI] pg/ml
Human	-	-	70-750	0-110
Human	+	-	4639 (6 x URL)	594 (5 x URL)
Human	+	+	5811 (8x URL)	910 (8 x URL)
Rats	-	-	100-460	0-180
Mice	-	-	159	2200

3.3.2 Clinical Presentation and Diagnosis

The early signs and symptoms of PPCM include orthopnea, hemptysis, palpitations, and cough. These symptoms coupled with an elevated blood pressure, increased jugular venous pressure, new murmurs of valvular regurgitation, and pulmonary rails are usually indicative of PPCM. A diagnosis requires an echocardiogram in which abnormalities such as sinus tachycardia, atrial fibrillation, abnormal voltage, prolonged PR and QRS intervals, and nonspecific ST and T wave changes are classic descriptors of PPCM(57).

3.3.3 Risk Factors and Causes

The risk factors and proposed causes of PPCM are outlined in Figure 1. The incidence of PPCM is greater in women of advanced maternal age, women with multiple gestations, or women of African American descent.

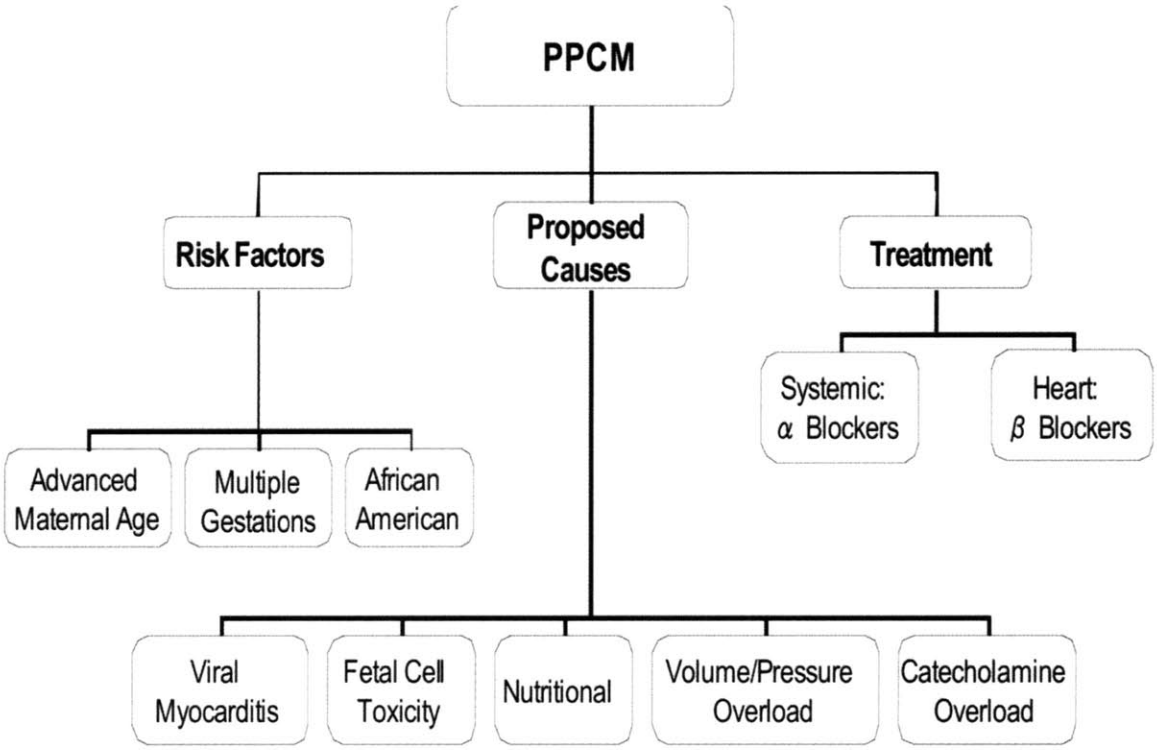

Figure 1. Risk Factors and Proposed Causes of Peripartum Cardiomyopathy.

3.3.4 Research, Current PPCM Models

Recent animal models of PICM have demonstrated the role of apoptosis and angiogenesis in the development of cardiomyopathy(58, 59). Hayawaka *et al.* demonstrated that transgenic mice over-expressing a subunit of Gα in the myocardium develop dilated cardiomyopathy that becomes lethal during pregnancy. Caspase inhibition ameliorates the cardiac dysfunction and suppresses mortality by 30%(59). These studies provide compelling evidence of the role of cardiomyocyte apoptosis in heart failure and introduce the possibility of caspase inhibition as a therapeutic agent. The role of apoptosis in PICM was further demonstrated in female mice with cardiomyocyte-specific knockout of STAT3, which developed PICM in a dose-dependent manner(58). STAT3 plays an important cardio-protective role via up-regulation of antioxidative enzymes and by promotion of myocardial angiogenesis.

3.4 Specific Aims

To date the understanding of the etiology and pathophysiology of peripartum cardiomyopathy lacks mechanistic rigor. It remains unknown as to whether peripartum cardiomyopathy with pheochromocytoma develops solely due to increased levels of catecholamines or to a combination of pheochromocytoma and pregnancy-related factors. Our experiments were designed to explore the underlying mechanisms of the rapid onset cardiomyopathies in pregnancy with or without concomitant pheochromocytoma. In addition to elucidating the pathophysiology and etiology of peripartum cardiomyopathy, this model serves as a paradigm for investigating the general mechanisms in disease progression.

Our specific thesis is that many diseases are dependent upon the complex interactions of multiple compounds and cofactors and that while one agent may dominate, its powerful effects are mediated through the synergistic action of the entire secretory cocktail. In this model we set out to investigate the ability of pheochromocytoma cells to induce cardiomyopathy in non-gravid, pseudo-gravid and gravid animals. We compared these data to the incidence of cardiomyopathy induced by infusion of catecholamines at doses equivalent to and in excess of what pheochromocytoma cells can generate.

We examined the synergistic interaction between pheochromocytoma cells within the physiologic milieu of pregnancy that resulted in rapid development of cardiomyopathy as a model of how auxiliary cell-secreted factors augment the potency of dominant agents and how this effect may be dependent on the physiologic status of

the host. A series of quantitative experiments that utilized rat models and tissue engineering compared cell-based versus catecholamine-induced cardiomyopathy in gravid, non-gravid and pseudo-gravid physiologic states. The specific aims of this thesis involve:

A. Isolation of the effect of catecholamines alone versus when they are accompanied by soluble factors released by the pheochromocytoma cells. This entailed the examination of the relative rates of induction of cardiomyopathy in rats implanted with catecholamine-releasing devices versus rats implanted with encapsulated pheochromocytoma cells. Functional assays of myocardial form and function were assessed with echocardiography and complemented by histological and immunohistochemical assessments of cardiac function.

B. Comparison of the rate and severity of onset of cardiomyopathy in non-gravid, gravid and pseudo-gravid rats implanted with catecholamine-releasing pumps and encapsulated pheochromocytoma cells.

By parsing out the effect of catecholamines alone vs. total pheochromocytoma cell secretions in gravid, pseudo-gravid and non-gravid animals, critical parameters underlying peripartum cardiomyopathy were characterized.

3.5 Scope of Work

This thesis seeks to dissect the general mechanism by which pheochromocytoma causes pathologic cardiac remodeling. Previous animal models of pheochromocytoma-induced cardiomyopathy implanted free pheochromocytoma cells whose unbridled growth lead to supra-physiological levels of catecholamines. The indication of cardiomyopathy was attributed to the high circulating levels of catecholamines, rare in patients exhibiting pheochromocytoma-induced cardiomyopathy. Thus a substantial portion of this work will focus on early grade pheochromocytomas secreting low levels of catecholamines. Chapter 4 details the development of polymeric encapsulation of pheochromocytoma cells essential to circumvent the unbridled tumor growth and catecholamine secretion seen in prior cell-implantation models. The polymer encapsulated pheochromocytoma cells secretory kinetics and cellular growth rate will be characterized *in vitro* and *in vivo*. The contractile and cytoskeletal effects of the polymer-encapulsated pheochromocytoma cells on isolated cardiomyocytes are demonstrated. Chapter 5 details the effects of implanted pheochromocytoma cells, norepinephrine secreting pumps and NE-deficient pheochromocytoma cells on cardiac function. These effects are demonstrated in two separate rodent models characterized by echocardiographic, gravimetric, invasive hemodynamic and histopathological analysis. The effects of the gravid state on the development of pheochromocytoma-induced cardiomyopathy is presented in Chapter 6. The cardiac function of gravid pheochromocytoma-bearing mice is serially tracked over a period of 56 days.

4 Encapsulated Pheochromocytoma Cells Secrete Potent Non-Catecholamine Factors

Abstract

Pheochromocytomas are widely believed to induce cardiomyopathy via hypersecretion of catecholamines including norepinephrine (NE). NE can have direct cardiomyocyte toxicity and/or can stimulate myocardial remodeling secondary to the induction of hypertension. Yet the development of cardiomyopathy is not entirely related to catecholamine dose or the extent of hypertension. To explore these effects, we engineered a polymeric encapsulation system to control PC12 cell kinetics and NE release *in vitro* and *in vivo*. Primary neonatal rat cardiomyocytes incubated with pheochromocytoma-conditioned media exhibited greater cytoskeletal changes than myocytes cultured with identical doses of NE alone, including more profound dose-dependent decreases in desmin, β-tubulin, and vinculin, and up-regulation of dystrophin. Cardiomyocyte contractility was 29 ± 6% greater at given levels of NE release. Agarose-encapsulated PC12 cells retain cell viability and structural integrity *in vivo*. These implants produced a 30% greater degree of cardiac enlargement compared to pumps releasing equivalent doses of NE. Protein level alterations observed *in vitro* were mirrored *in vivo* following implantation of encapsulated cells or NE pumps for 28 days. Together, these data suggest that pheochromocytoma-induced cardiomyopathy is not solely a catecholamine-mediated event; rather the pathogenesis of this dilated cardiomyopathy appears to be dependent upon secondary factors unexamined to date.

4.1 Introduction

Pheochromocytomas are catecholamine-producing neuroendocrine tumors arising from chromaffin cells of the adrenal medulla or extra-adrenal paraganglia. The tumor products, including catecholamines, induce significant systemic pathology in addition to local invasive pathology. Clinical presentation is highly variable. Some patients exhibit dramatic hemodynamic effects while others remain unaffected by "silent" tumors (46). One particularly devastating consequence of tumor secretion is dilated cardiomyopathy which often progresses to congestive heart failure (60). Though infrequent, pheochromocytoma-induced cardiomyopathy provides an excellent model for examining issues related to specific etiology and the relative contributions of interrelated factors in the pathogenesis of disease. Pheochromocytomas are characterized by neoplastic hypersecretion of catecholamines, predominantly or exclusively norepinephrine (NE), and, to a much lesser extent, its metabolite epinephrine (61-64). These compounds can induce cardiotoxic effects and dilated cardiomyopathy in model systems. PICM has been traditionally viewed as a solely catecholamine-mediated disease process. Yet other known secretory products of pheochromocytomas, such as TGF-ß and IL-6, are themselves cardiotoxic and may modulate the development of cardiomyopathy even in the absence of catecholamines (40, 42-45).

Clinical experience also questions this assumption: up to 36% of patients with pheochromocytomas exhibit no hypertension or abnormal catecholamine levels but still develop PICM (46, 65). This clinical paradox, together with data suggesting the potency

of non-catecholamine endocrine factors in the pathogenesis of cardiomyopathy, led us to hypothesize that the cardiotoxic effects of pheochromocytomas are not solely catecholamine-mediated; rather a complex of tumor-secreted factors modulates cardiomyocyte remodeling even at non-cardiotoxic levels of catecholamines.

Previous attempts to draw a direct comparison between the effects of pheochromocytomas and NE alone *in vivo* have been hindered by a lack of control over catecholamine secretion rate, resulting in supra-physiologic levels of circulating NE (65). These models not only invariably induce cardiomyopathy but may also mask secondary factors at work. While these models yield insight into the role of catecholamines in PICM, they fail to explain the progression of disease in patients with undetectable or low degrees of catecholamine elevation (65), as well as the reversibility of PICM seen in early-stage pheochromocytoma patients (42, 66-70).

To explore the effects of NE alone versus pheochromocytoma-secreted factors, neonatal rat cardiomyocytes were exposed to NE or conditioned media of pheochromocytoma (PC12) cells while tracking contractility and cytoskeletal remodeling. An *in vivo* model was also developed using controlled-release of pheochromocytoma factors or NE. Tumor secretions increased the contractility of, and induced greater remodeling effects on, isolated cardiomyocytes than equivalent doses of NE alone, and had similar effects on hearts *in situ* when cells and NE pumps were implanted *in vivo*. The effects of tumor secretions outweighed those of NE alone in cardiomyocyte and cardiac function and remodeling. Such findings validate the

synergistic effects of pheochromocytoma-secreted products with catecholamines in general and speak to the more general etiology of cardiomyopathy and tumor pathology.

4.2 Materials and Methods

4.2.1 Cell Culture and Characterization

Rat pheochromocytoma cells (PC12, ATCC, VA) were cultured in F12K media (ATCC) with 10% horse serum (Hyclone, UT), 5% FBS (Hyclone), and 100 units/ml penicillin/streptomyocin (Invitrogen, CA) (25). Mouse pheochromocytoma cells (MPC 4/30/PRR, kindly provided by Dr. Tischler, New England Medical Center, MA) were maintained in RPMI 1640 media (Invitrogen) with 10% horse serum (Hyclone), 5% FBS (Hyclone), and 100 units/ml penicillin/streptomyocin (Invitrogen) (48). Both cell lines were grown at 37°C, 5% CO2, and were passaged every two days.

4.2.2 Preparation and characterization of microspheres

PLG microspheres were prepared by solvent evaporation method. Poly(DL-lactide-co-glycolide) (65:35, Durect, Pelham, AL) (200 mg) was suspended in 4 ml of dichloromethane (Sigma). Then 20 mg of norepinephrine (Sigma) was added to polymer solution and sonicated for 10 min. A primary emulsion was prepared by adding 2 ml of 5% PVA solution to the polymer solution and homogenized for 30 seconds with occasional vortexing to cause complete dissolution of the polymer in the organic phase. This emulsion was then added slowly to 1% PVA solution (100 ml) drop-wise and stirred at a constant speed (250–300 rpm) for 3 h at room temperature for complete evaporation of the organic solvent. The formed microspheres were then filtered and washed with distilled de-ionized water and snap frozen for storage.

2.2.1.2. NE Release from DL-PLG Microspheres

Microspheres (5 mg) were incubated in 10 mL acidic saline (50 µg/mL ascorbic acid in PBS) and stored at 37°C/ 5% CO_2. Daily 500 µL of media was removed and NE measured by ELISA (Rocky Mountain Diagnostics). Studies were conducted from three separate batches.

4.2.3 Preparation and Validation of Mini Osmotic Pumps

Osmotic pumps (Alzet, Model 2004, CA) delivering 0.25 µL/hr were loaded with 9.06 µM solution of NE in acidic saline (0.1mg/mL ascorbic acid in saline). As validation of their release rate a total of three mini osmotic pumps loaded with NE were individually incubated in 50 mL acidic saline (50 µg/mL ascorbic acid in PBS) and stored at 37°C/ 5% CO_2. Daily 500 µL of media was removed and NE measured by ELISA (Rocky Mountain Diagnostics). Studies were conducted from three separate batches.

4.2.4 Design of Polymeric Encapsulation Device

To better understand the microenvironment within a cell-implanted agarose bead and to determine the optimal seeding conditions and size, a mathematical model of the oxygen concentration profile within the bead was developed based upon mass transfer equations. The model is centered on a 0^{th} order differential equation accounting for oxygen diffusion and consumption. Assuming the system has reached steady state and the only variations in oxygen concentration are in the radial direction, oxygen concentration within the bead can be modeled as $C(r) = C_o + \frac{ka}{6D}(r^2 - b^2)$ where, C(r) = oxygen concentration at r(m) from the center of the bead [moles/L], C_o = bulk oxygen

concentration [moles/L], k = oxygen consumption rate [moles/cell*s], b = bead diameter [m], a = cell density per bead [cells/mL] and D = oxygen diffusivity in agarose bead [m^2/s]. Simulations were carried out using Matlab (Mathworks, Natick, MA) with parameters from the literature; $k=8.67 \times 10^{-17}$ moles/cell*s, $D = 2x10^{-9}$ m^2/s (71) and $C_o = 9x10^{-4}$ M/L (72). The boundary conditions for the system included setting the O_2 concentration at outer bead boundary to the bulk O_2 concentration and no change in O_2 concentration at the bead's core. The oxygen concentration profile simulations calculated the optimal cell density and bead diameter necessary to maintain uniform cell viability. The minimum oxygen concentration profile (dashed line Figure 2) was based on previous studies regarding the minimum oxygen requirements of rat neonatal cell aggregates(73). A projected optimal bead size of 2.67 mm in diameter maintained uniform oxygen concentration. Cellular densities greater than $4x10^6$ cells/mL were disadvantageous as oxygen concentration dropped dramatically in regions of the bead far from the surface (Figure 2).

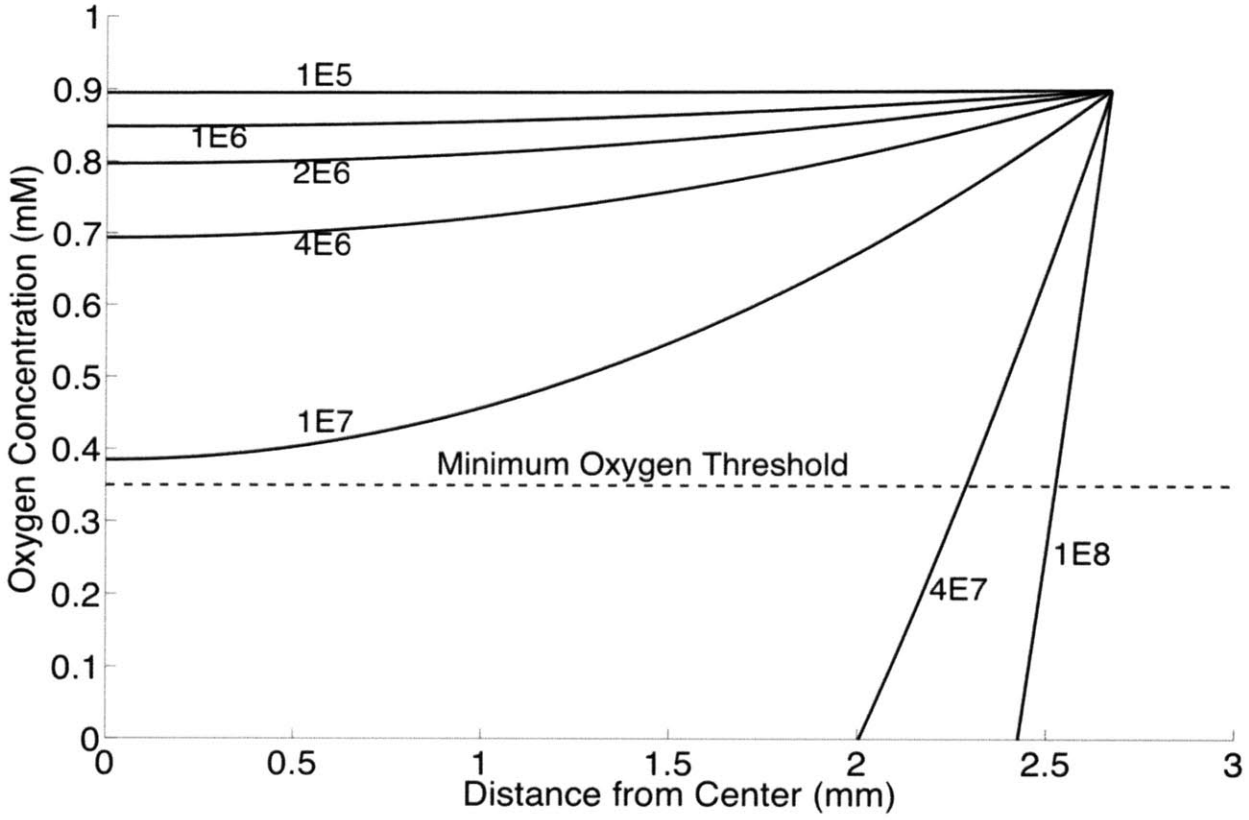

Figure 2. Simulated oxygen concentration profile for agarose encapsulated PC12 cells. Each line represents the encapsulation density of PC12 cells (cells/mL). The dashed line represents the minimum oxygen requirements of rat neonatal cell aggregates.

4.2.5 Cardiomyocyte Isolation and Contractility

Cardiomyocytes were obtained from the ventricles of two-day old neonatal rats using established methods (74) under an institute-approved protocol. Freshly isolated cells were pre-plated for 60 minutes to enrich for cardiomyocytes, and then plated 3 x 10^5 cells/cm^2 in laminin-coated 60 mm petri dishes. Culture media was conditioned by secretions of PC12 cells using beads of agarose-encapsulated PC12 and determining equivalent NE concentrations, based on drug delivery studies. Identical controls were cultured in media supplemented with NE. On culture day four, contractility was assessed on auto-contracting cardiomyocytes using an optically transparent, environmentally controlled test chamber, an inverted microscope (Zeiss Axiovert 200M), and a digital video camera (Sony XCD-X710, Tokyo, Japan). Machine visual screening software (Visible Discovery; Reify Corp., MA) calculated the aggregate change index (ACI), a measure of contractility-induced change in the spatial organization of light intensity (i.e., a measure of contractile amplitude) (75). The contractile frequency of cardiomyocytes was quantified as the mean value of the peaks of the ACI for each concentration. The ACI function does not require image segmentation and therefore is applicable to high-density neonatal cardiomyocyte cultures in which cell edges cannot be readily localized.

4.2.6 Cardiomyocyte Protein Analysis

Confluent cardiomyocytes were scraped off TCPS, counted, aliquoted, ($1x10^6$ cells/vial) and incubated with lysis solution (20 mM Tris, 150 mM NaCl, 1% Triton X-100, 0.1% SDS, 2 mM sodium orthovanadate, 2 mM PMSF, 50 mM NaF, protease inhibitor cocktail, Roche). Samples were boiled for 5 minutes with Laemmli sample buffer and separated on Nupage gels (Invitrogen). Cardiomyocytes incubated in growth media without PC12-conditioned media or norepinephrine served as controls. Proteins were transferred onto membranes using iBlot stacks (Invitrogen), blocked and incubated with dystrophin polyclonal (Abcam), desmin polyclonal (Abcam), β-tubulin monoclonal (Abcam), or RPL32 polyclonal (Aviva Systems Biology, CA) antibody. Membranes were incubated with a goat anti-rabbit or goat anti-mouse monoclonal antibody (Santa Cruz Biotechnology, CA) at a 1:1000 dilution for two hours at room temperature. The membranes were then washed in PBS-T (PBS with 0.05% Tween 20) and incubated with the Western Supersignal Femto kit (Pierce, IL). The membranes were exposed on a FluorChem SP (Alpha Innotech, CA).

4.2.7 Encapsulation and Survival of MPC and PC12 Cells in Agarose Beads

Agarose beads were developed as previously described(76). PC12 cells were scraped, centrifuged, and re-suspended in a preheated solution of 2.5% (w/w) agarose (Sigma–Aldrich, Type VII, MO) in 0.9% NaCl. The mixture was drawn into a pipette and 10 µL aliquots sheared into a mineral oil bath (~600 mL). The beads were separated using a 1,000 mm pore size nylon mesh (Small Parts, FL) and washed with PBS. Cell proliferation within agarose bead was assayed with 3-(4,5-dimethylthiazol-2-yl)-2,5-

diphenyltetrazolium bromide (Sigma) per manufacturer instructions. The optical density was read on a microplate photometer (BioTek Instruments, VT) and compared to a standard curve with known numbers of PC12 cells. Epinephrine, norepinephrine, and dopamine secretion rate was assayed daily from media containing agarose-encapsulated cells by ELISA (Rocky Mountain Diagnostics, CO). Ascorbic acid (50 μg/mL) was added to the media to minimize oxidation of catecholamines.

4.2.8 Animal Experiments

Female Sprague-Dawley rats (8 weeks old, 250 gm) were obtained from Charles River (MA). A total of twenty PC12-encapsulated agarose beads were implanted in the retro-peritoneal cavity adjacent to the kidneys, to mimic the spatial release of pheochromocytoma cells, for an overall secretion rate of 9.2 ng/day. Osmotic pumps (Alzet, Model 2004, CA) delivering 0.25 μL/hr were loaded with 9.06 μM solution of NE in acidic saline (0.1mg/mL ascorbic acid in saline). Control animals received osmotic pumps loaded with the ascorbic acid/saline solution. No statistical difference in cardiac function was found in rats implanted with empty agarose beads and non-surgical, non-implanted rats. All animal studies were performed in accordance with protocols approved by the IACUC at the Massachusetts Institute of Technology. Existing catecholamine levels in the rats were tracked weekly with blood draws via the retro-orbital plexus. Plasma catecholamines were quantified by ELISA (Rocky Mountain Diagnostics).

4.2.9 Cardiomyocyte Protein Extraction

Hearts were excised, washed in PBS, and the LV was separated and frozen in liquid nitrogen. Sections (2x2x2 mm) were weighed and sectioned in a microtome and lysed in 1 mL solution (20 mM Tris, 150 mM NaCl, NaOH pH 8.0, pH with NaOH, 1% Triton X-100, 0.1% SDS, 2 mM sodium orthovanadate, 2 mM PMSF, 50 mM NaF, protease inhibitor cocktail, Roche). Proteins were isolated as described above. Membranes were incubated with dystrophin polyclonal antibody (Abcam), desmin polyclonal antibody (Abcam), β-tubulin monoclonal antibody (Abcam), or RPL32 polyclonal antibody (Aviva Systems Biology). The secondary antibodies used were goat anti-rabbit or goat anti-mouse monoclonal antibody (Santa Cruz Biotechnology) at a 1:1,000 dilution.

4.2.10 Histology

Rat hearts were excised, rinsed in PBS, blotted dry, and weighed. The hearts were then pressure perfused with PBS for 5 minutes followed by perfusion with 10% neutral buffered formalin (NBF) until interpreted as visibly firm and pale. The hearts were placed in 10% NBF for 18 hours, subsequently processed, fixed in paraffin (Polysciences Inc., PA), and serial coronal sections were cut and stained with Masson's Trichrome (American HistoLabs Inc., MD).

4.2.11 RNA Preparation, Semi-quantitative RT-PCR

Isolated hearts were excised and perfused with PBS (Invitrogen) for 5 minutes. A biopsy punch was used to section out an 8 x 8 x 8mm section of the left ventricle. Total RNA was isolated with the use of Qiashredder and RNeasy spin columns, including chromosomal DNase digestion (Qiagen, CA). Twenty micrograms of total RNA were reverse transcribed into cDNA with the use of oligo(dT)24 primers containing a T7 RNA polymerase promoter. First-strand cDNA was synthesized using Taqman RT-PCR kit (Applied Biosystems, CA). Specific primers were designed using Primer3 (77). Real-time polymerase chain reaction (PCR) analysis was performed with an Opticon Real Time PCR Machine (Biorad, CA) using SYBR Green PCR Master Mix (Applied Biosystems). The resulting data were analyzed with the complementary Opticon computer software (Biorad). All samples (n=5 per group) were measured in triplicate and the expression level was normalized to GAPDH expression.

4.3 Results

4.3.1 NE Encapsulation in DL-PLG Microspheres

Production of norepinephrine loaded DL-PLGA microspheres resulted in a yield of 50 – 70% viable microspheres. The resulting end product, as visualized by light microscopy, was an opaque powder, with minimal aggregation. DL-PLGA microspheres were synthesized with mean diameters ranging from 100 – 300 μm, depending on the amount of time the particle solution was sonicated and homogenized. Each particle diameter possessed separate NE release kinetics (Figure 3). The 600 μm beads demonstrated the most stable NE release rate and reproducibility compared to the 100 and 300 μm beads.

The beads demonstrated a bulk release of NE over the first 3 days of release, with the degradation settling to a stable rate by day 4 and dropping significantly following 18 days in culture.

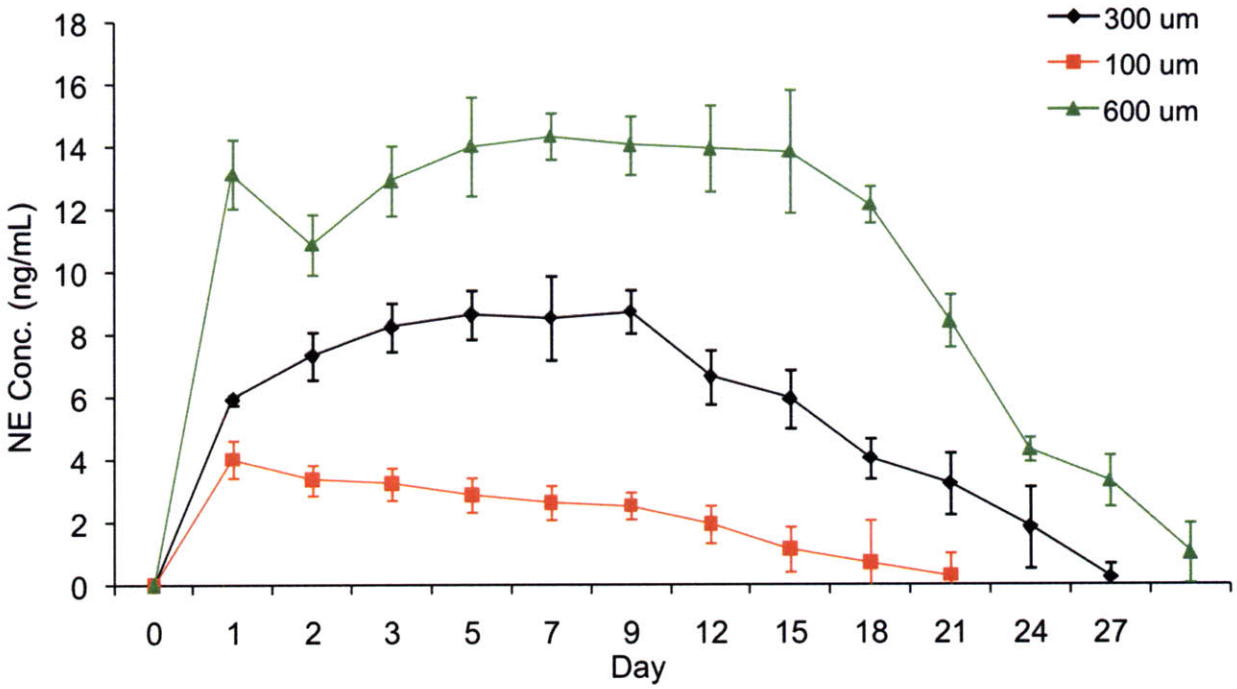

Figure 3. Temporal norepinephrine release from DL-PLG biodegradable microspheres. NE release from DL-PLG microspheres was quantified for a series of beads; 100 μm, 300 μm and 600 μm diameter. Results presented as mean ± SE.

4.3.2 Norepinephrine Releasing Mini Osmotic Pump Validation

Norepinephrine secreting mini osmotic pumps secreted a stable level of norepinephrine for a period of 26 days (Figure 4). The norepinephrine secreted by the pumps deviated little over the entire period of study and was highly replicated in each successive study.

The mini osmotic pumps provide continual release of norepinephrine mimicking the physiological release of norepinephrine by pheochromocytomas and the adrenal glands. Implantation in the peritoneal cavity should replicate secretion by implanted pheochromocytoma cells without the entire pheochromocytoma secretome.

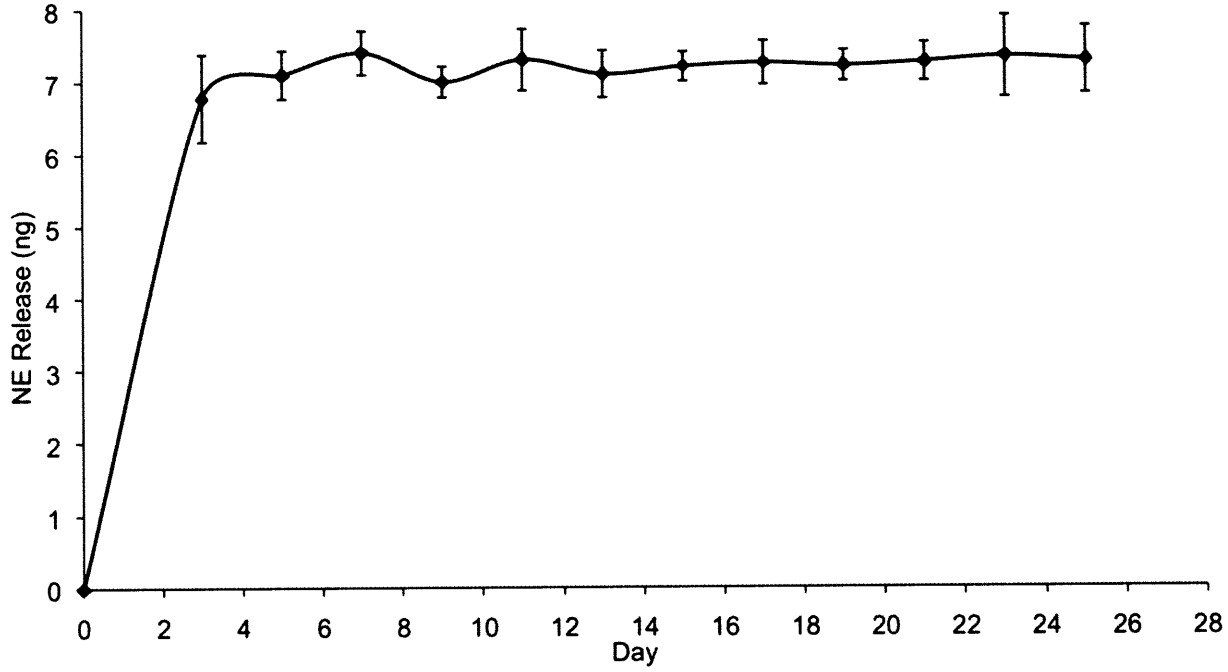

Figure 4. Norepinephrine secretion from mini osmotic pump for a period of 26 days.

Results presented as mean ± SD.

4.3.3 Agarose Encapsulation of MPC and PC12 Cells

Mouse (MPC, Figure 5, A) and rat pheochromocytoma cells (PC12, Figure 5, B) were encapsulated in agarose beads. Both cells continued to grow after encapsulation and released quantifiable levels of catecholamines. Whereas encapsulated PC12 cells retained a narrow range of cell number and NE release (Figure 5, D, F), MPC cells were less viable and the NE release highly variable *in vivo* (Figure 5, C, E). Dopamine levels in PC12 cells were undetectable(78), as were epinephrine levels given the low or non-existent expression of phenylethanolamine-N-methyltransferase, the enzyme responsible for converting norepinephrine to epinephrine(49). The lack of epinephrine or dopamine secretion makes PC12 cells then an ideal side-by-side comparison to the NE-secreting pumps. Varying formulations of agarose beads were evaluated, including the addition of collagen and use of cell aggregates, to optimize cell growth and secretory function. Addition of collagen and use of cell aggregates induced minimal changes in their secretory ability (Figure 5,G). Agarose-encapsulated PC12 cells at a density of $4x10^6$ cells/mL maintained similar growth kinetics and metabolism to PC12 cells grown on polystyrene dishes (TCPS) (Figure 5,H). NE secretion from encapsulated cells (29.24±1.09 ng) was statistically indistinguishable from cells cultured on TCPS (30.29±0.73 ng, $p>0.05$).

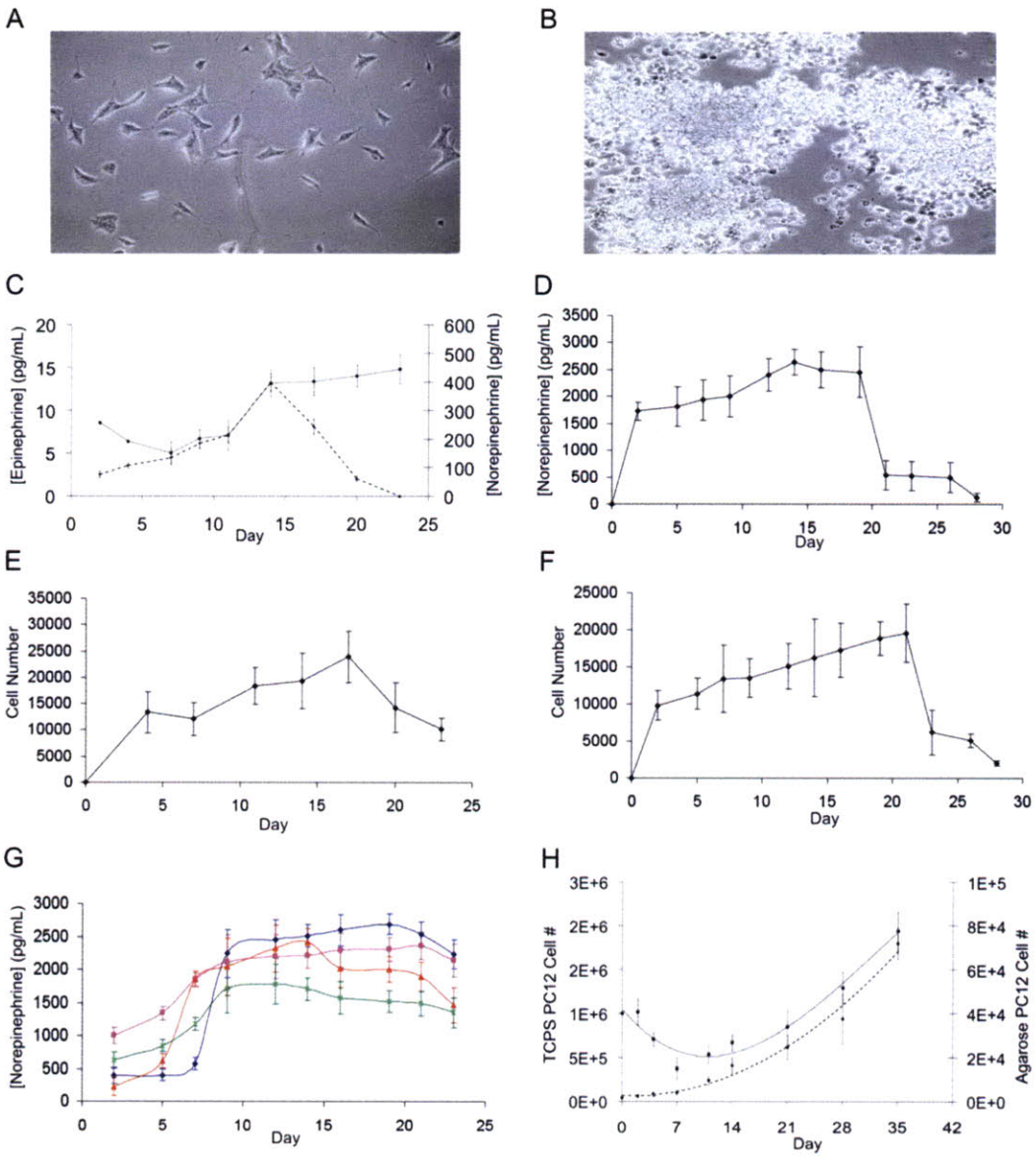

Figure 5. Encapsulation of MPC and PC12 cells does not affect their growth or secretory ability. Representative images of MPC cells (A) and PC12 cells (B). Norepinephrine release profile for agarose encapsulated MPC cells (4x106 cells/ bead, epinephrine = grey line, norepinephrine = black line) (C) and PC12 cells (4x106 cells/ bead) (D). Cell growth kinetics for agarose-encapsulated MPC cells (E) and PC12 cells (F). Norepinephrine release profile for different formulations of agarose encapsulation (G), (blue = 2.5% agarose, pink = 2.5% agarose with 25% collagen, red = PC12 cells in aggregates, green = 40% collagen). (H) Comparison of PC12 cell growth within agarose beads (4x104 cells/ bead, black line) versus PC12 cells cultured on TCPS dishes (grey line). All plots are mean ± SD, n=4.

4.3.4 Cardiomyocyte Cytoskeletal Contractility and Remodeling

Primary neonatal rat cardiomyocytes were incubated with either PC12-conditioned or NE-containing media. NE induced a dose-dependent increase in cardiomyocyte contraction force and frequency (Figure 6, A, B). Encapsulated PC12-conditioned media exhibited similar increases in contractility to equivalent NE doses below 0.1 nM, but significantly greater increases at doses of 0.1 to 0.5 nM, and greater reductions of contractility than NE-only counterparts at 1 and 10 nM (Figure 6, B). PC-12 conditioned media induced almost two-fold greater contractility at 0.1 nM NE ($p<0.01$). The altered chronotropic effects of PC12-conditioned media versus identical doses of NE were dose-dependent. Expression of cytoskeletal proteins followed suit (Figure 7**).** The dose dependent effects of NE were enhanced by PC12-conditioned media; desmin (-35 ± 8% vs. -22 ± 7%), β-tubulin (-34 ± 9% vs. 8 ± 12%), and vinculin (34 ± 5% vs. 1 ± 3%) were all reduced and Dystrophin increased to a greater extent at the lower levels of NE release by the PC12 media.

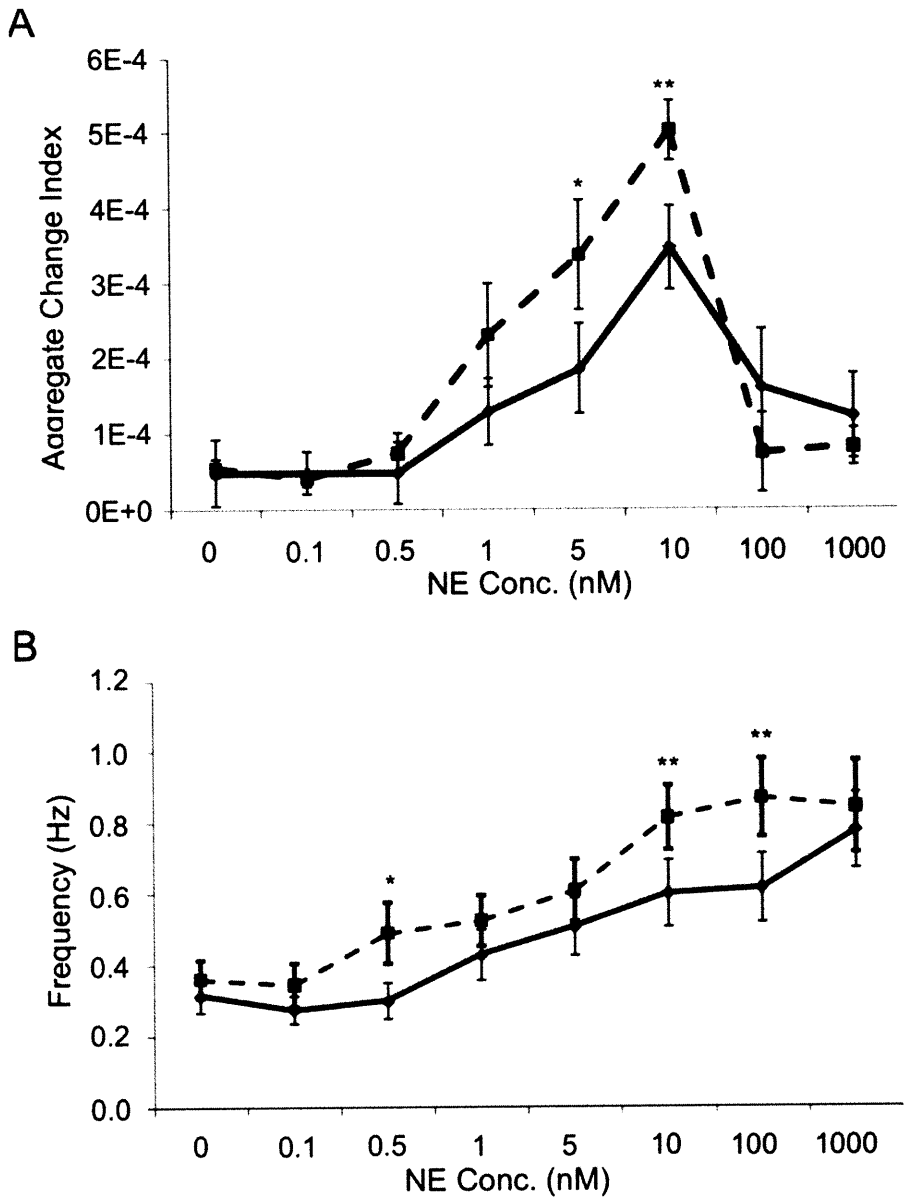

Figure 6. PC12-conditioned media induces a greater contractile effect on cardiomyocytes than identical doses of NE alone. (A) Aggregate change index for cardiomyocytes incubated with PC12-conditioned media (grey) or identical concentrations of NE alone (black). (B) Frequency of cardiomyocyte contraction. The data at each time point is the mean ± SD of n= 3 separate culture plates. * $P<0.05$,

** $P<0.01$ for PC12-media vs. NE.

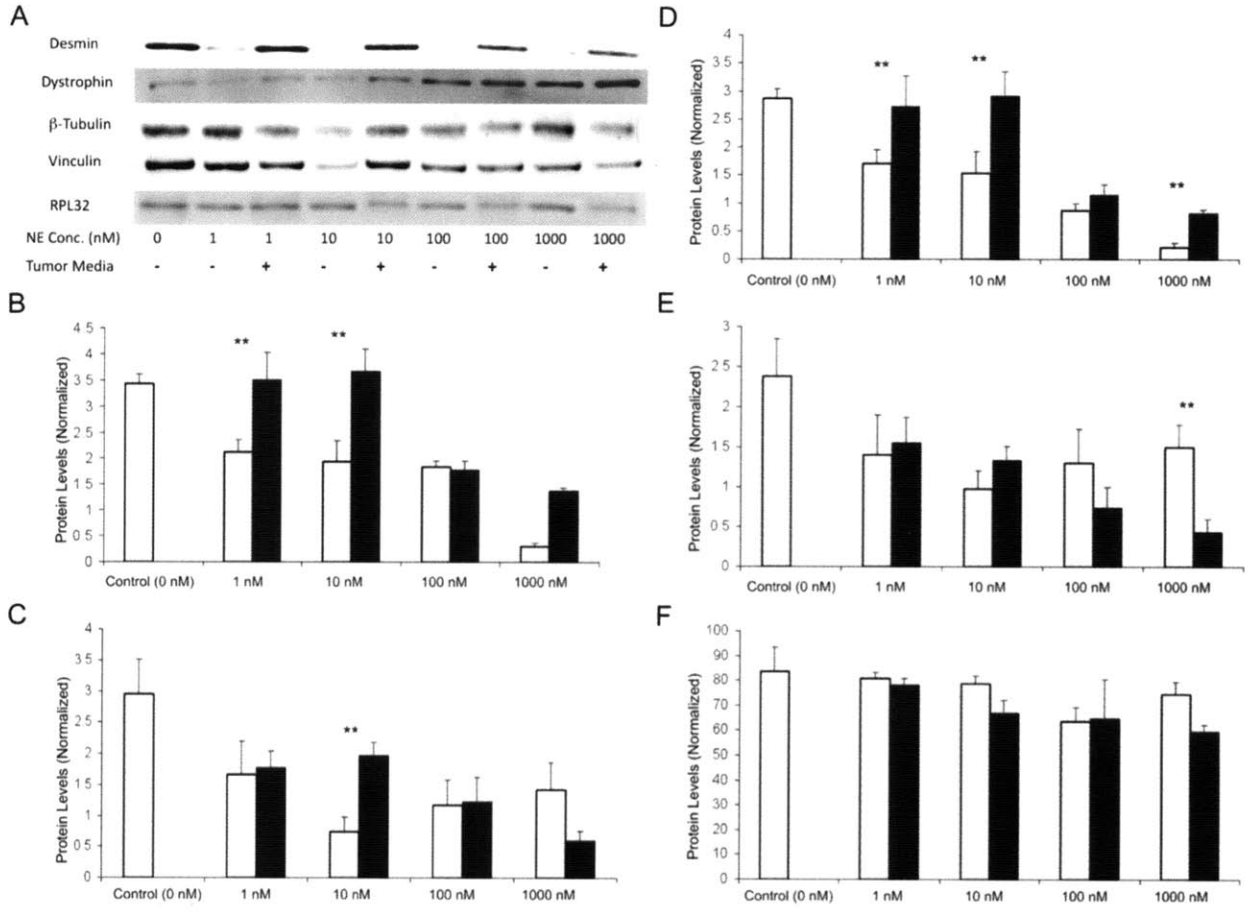

Figure 7. Cardiomyocytes incubated with PC12-conditioned media undergo differential cardiomyocyte remodeling from those incubated with identical doses of NE alone. (A) Comparison of protein levels in cardiomyocytes incubated with PC12-conditioned media versus identical doses of NE media. Densitometry analysis normalized to RPL32 levels for (B) desmin, (C) dystrophin, (D) β-tubulin, (E) vinculin, and (F) RPL32. * $P<0.05$, ** $P<0.01$ for PC12-media vs. NE.

4.3.5 *In Vivo* Model and Cardiac Morphology

Preliminary data showed that encapsulated PC12 cells survived longer and secreted greater levels of NE than encapsulated MPC cells for the time period of interest; encapsulated PC12 cells were therefore used in subsequent animal studies. Implantation of agarose-encapsulated PC12 cells in the retroperitoneal cavity of rats demonstrated the ability of PC12 cells to secrete catecholamines *in vivo* without eliciting an immune reaction. Histological analysis revealed the formation of a fibrous capsule (120 μm) at the bead surface, which did not inhibit their secretory ability, based on circulating plasma NE levels (Figure 9, E, F). Norepinephrine-secreting osmotic pumps were implanted to match the NE secretory rate of implanted encapsulated PC12 constructs. As validation of our delivery methods the implantation of osmotic pumps secreting 9.2 ng NE per day induced an increase in plasma NE concentration by 310 ± 62 pg/mL in rats. Similarly, agarose-encapsulated PC12 cells secreting 9.2 ng NE per day increased plasma NE concentration by 250 ± 49 ng/mL in rats (Figure 8, A).

Heart weight normalized to body weight was used as a measure of cardiac remodeling following 28-day implantation. The hearts of Pheo animals were 31% larger than controls ($p<0.01$) and 20% greater than NE rats ($p<0.01$); the latter statistically indistinguishable from controls (Figure 8, B). Brain natriuretic peptide (BNP) and its precursor, proBNP, is released from the cardiac ventricles in response to pressure overload, particularly in the context of heart failure (79) (80). proBNP and BNP mRNA levels were elevated 250 ± 35% and 280 ± 20% respectively, above control rats 28 days

after implantation. Rats implanted with NE pumps secreting identical doses of NE exhibited mRNA levels indistinguishable from controls (78 ± 12% and 68 ± 11% versus controls). These statistically significant changes highlight the ability of pheochromocytomas to induce cardiac pathology with accelerated kinetics versus catecholamines alone. Histological analyses of cardiac tissue showed greater fibrosis, vessel hemorrhage, and myofiber necrosis in Pheo versus NE and control rats (Figure 9, A-D).

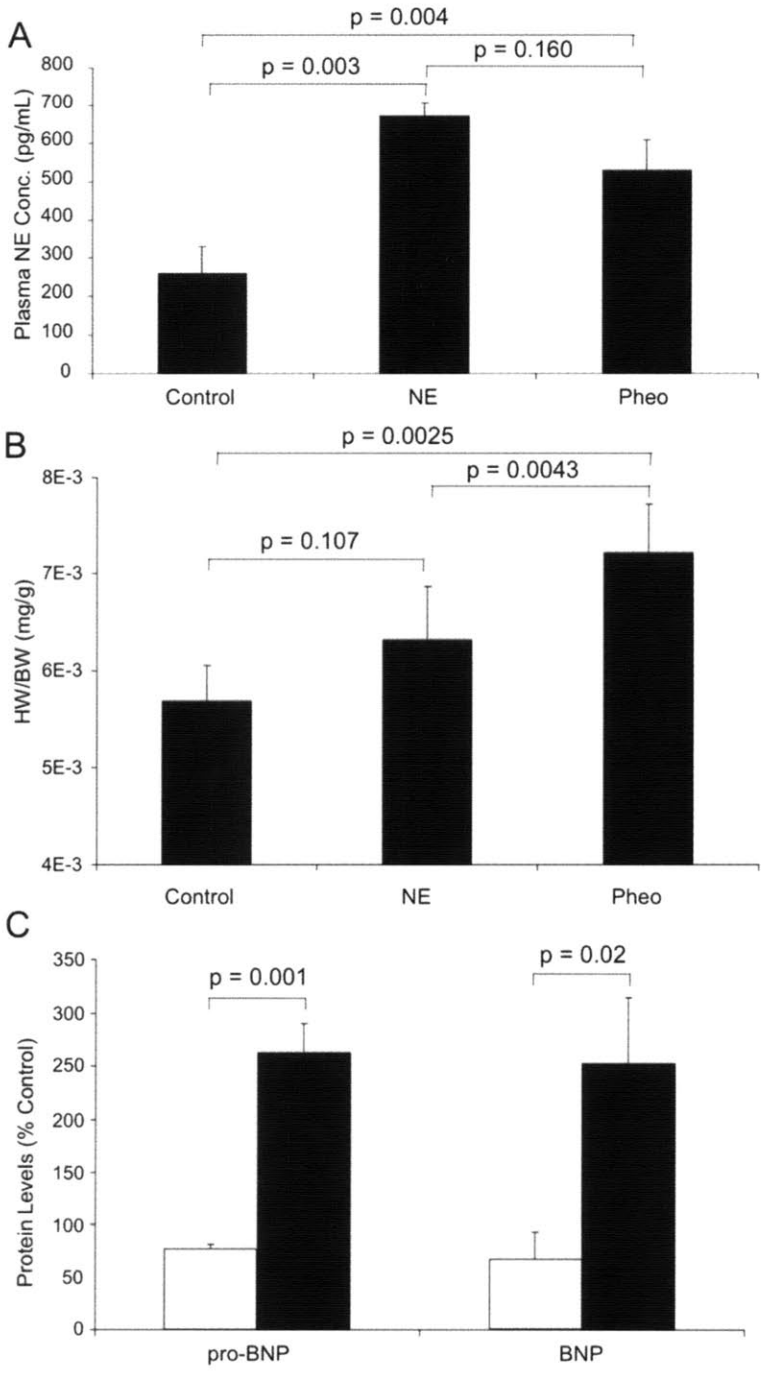

Figure 8. Agarose-encapsulated PC12 cells retain cellular integrity, secretory ability, and induce cardiac pathology. (A) Plasma catecholamine concentrations in rats with peritoneally-implanted agarose-encapsulated PC12 cells or NE pumps were comparably elevated on day 28. (B) Heart weight to body weight ratio was elevated in PC12-implanted rats on day 28, but not significantly in NE-pump implanted rats. (C) LV mRNA levels in rats implanted with PC12 cells (black bar) or NE secreting pumps (grey bars) after 28 days of implantation.

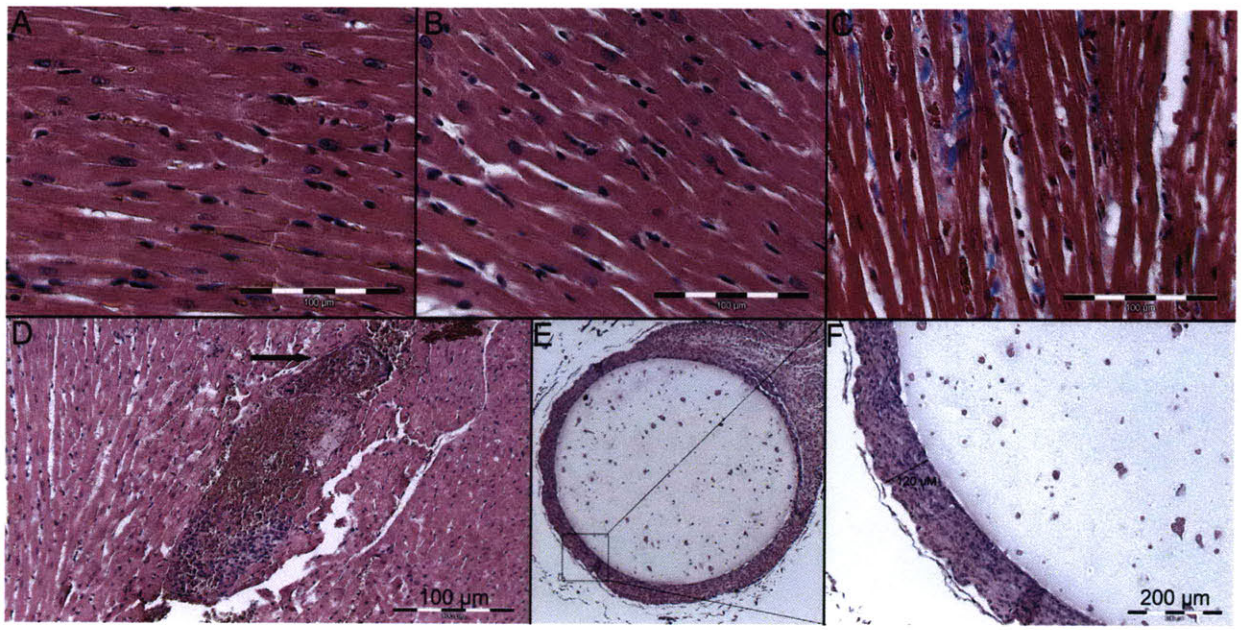

Figure 9. Implanted pheochromocytoma cells induce cardiac pathology suggestive of dilated cardiomyopathy. Representative left ventricular light microscopy image of control (A), NE-treated (B), and PC12-implanted left ventricle (C) stained with Masson's Trichrome at day 28. Images at 20x magnification, scale bar represents 100 mm. (D) Arrow indicates hemorrhaging vessel seen in pheochromocytoma-implanted rat. (E) Representative light microscopy image of explanted PC12-containing agarose beads stained with H&E at day 28. (F) Higher magnification of (E). Note minimal formation of fibrous capsule and absence of inflammatory infiltrate.

4.3.6 *In Vivo* Cell and Pump Release Kinetics and Effects on Cardiac Function and Cytoskeleton

Agarose-encapsulated PC12 cells or osmotic pumps secreting 9.2 ng NE per day were implanted retro-peritoneally in rats for 28 days. Cytoskeletal protein expression changed *in vivo* as it had in culture, with greatest reductions in all proteins in cell-implanted rats and to a greater extent than equivalent amounts of NE alone. PC12-implanted rats exhibited greatest changes in these proteins; desmin (30 ± 7% decrease vs. control, 31 ± 9% decrease vs. NE), β-tubulin (80 ± 15 % decrease vs. control, 77 ± 9% decrease vs. NE), dystrophin (23 ± 9% decrease vs. control, 9 ± 2% decrease vs. NE), and vinculin (26 ± 11% decrease, 19 ± 9% decrease vs. NE; Figure 10).

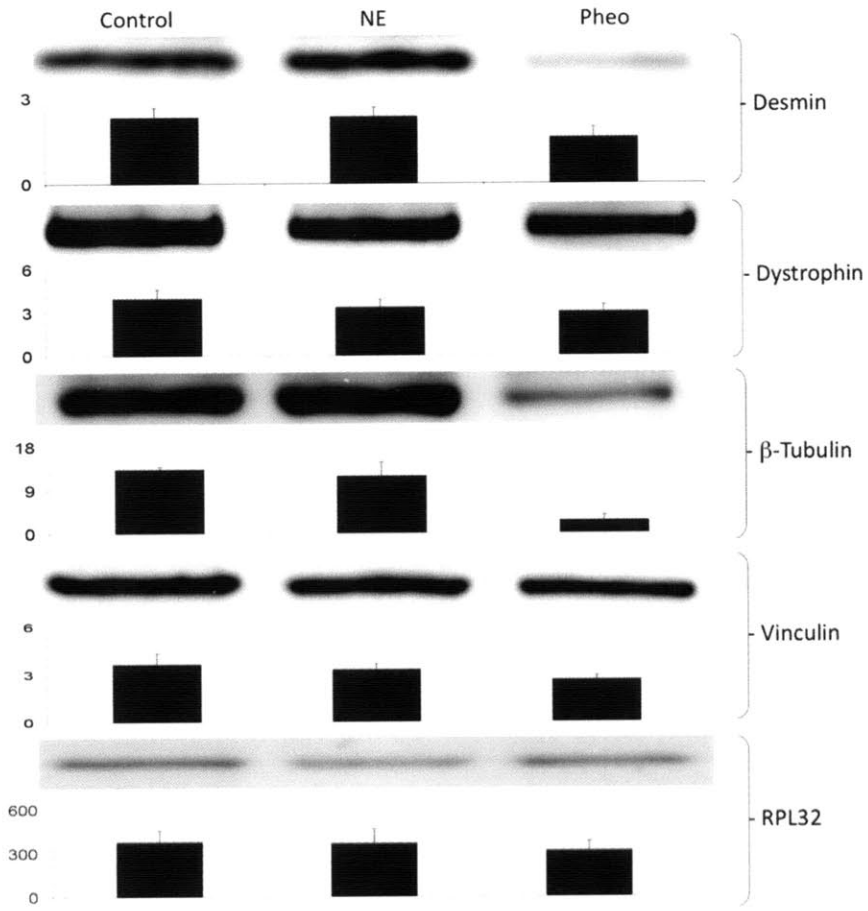

Figure 10. Implanted pheochromocytoma cells induce cardiomyocyte remodeling similar to in vitro observations. Cardiac protein levels after implantation of agarose-encapsulated PC12 cells and NE-secreting pumps for 28 days. Each western blot is followed by a densitometry analysis normalized to RPL32 density. Rats implanted with NE-secreting pumps exhibited desmin levels similar to controls (1 ± 2 % increase vs. control), while β-tubulin, vinculin and dystrophin levels decreased (10 ± 3 % vs. control, 9 ± 2 % vs. control, and 16 ± 4 % average, respectively). Rats with PC12 implants exhibited decreases in all four proteins relative to controls (desmin 30 ± 7%, dystrophin 23 ± 9%, β-tubulin 80 ± 15%, and vinculin 26 ± 11%) vs. RPL-normalized controls).

Table 2. PC-12 conditioned media induces coordinated alterations in contractile apparatus proteins.

Proteins Correlated	Pheo-Conditioned Media (r)	NE-Conditioned Media (r)	Implanted PC12 (r)
ß-tubulin/Desmin	0.857	0.031	0.988
ß-tubulin/Dystrophin	0.903	0.094	0.823
ß-tubulin/Vinculin	0.976	0.573	0.973
Desmin/Dystrophin	0.968	0.937	0.725
Desmin/Vinculin	0.859	0.221	0.926
Dystrophin/Vinculin	0.874	0.447	0.932

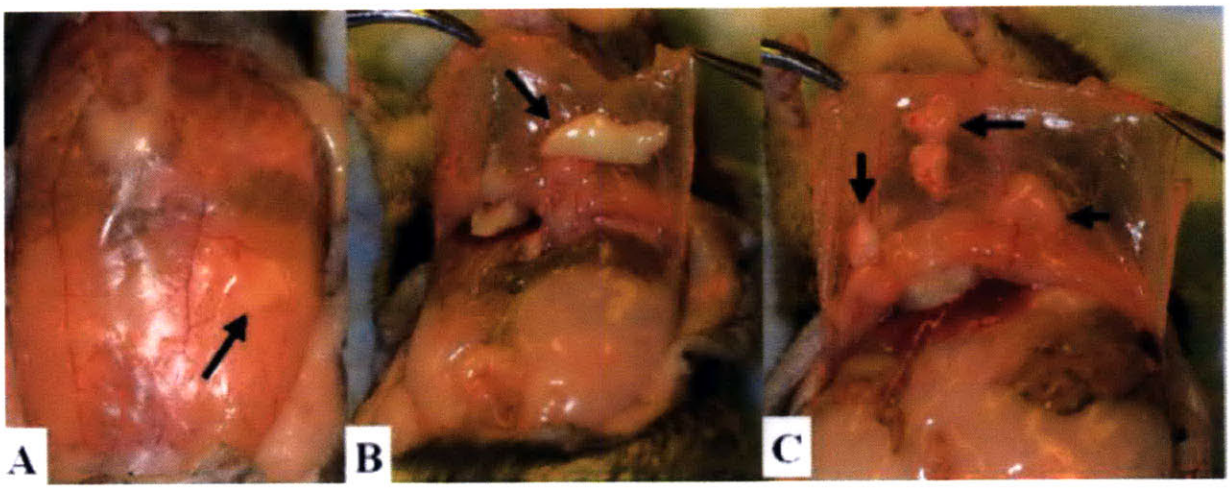

Figure 11. DL-PLGA microparticle residue in the peritoneum (arrows), 2 weeks after injection. (A) Depicts microsphere residue as seen through the abdominal wall in a mouse. (B-C) Highlight the fibrous encapsulated microspheres.

Ref: Kohane et. al. / J Biomed Mater Res 77A: 351–361, 2006

4.4 Discussion

To the best of our knowledge this study is the first to analyze the direct impact of NE versus the complete complex of factors secreted by pheochromocytomas on primary cardiomyocyte physiology. Traditional models of PICM have relied upon the implantation of free PC12 cells resulting in uncontrolled cell growth and release of catecholamines (18, 65). Although these studies provided important information on the cardiotoxic effects of catecholamines and the ability of large pheochromocytomas to induce cardiomyopathy, the magnitude of NE released may have masked the effects of secondary factors secreted by these tumors. Moreover, the rapid growth of injected free PC12 cells renders them unsuitable in the study of nascent tumors, which often induce cardiomyopathy in the context of low levels of catecholamines.

Pheochromocytomas have long been postulated to induce cardiomyopathy via hypersecretion of catecholamines. Excessive adrenergic stimulation has been established as cardiotoxic in multiple species. Mann et al. demonstrated the dose-dependent effects of NE resulting in increased cell death, decreased protein synthetic ability, and altered cardiomyocyte morphology suggestive of decreased contractility (37). But the pheochromocytoma secretome also includes other known cardiotoxic factors, including TGF-ß and IL-6. Limited data show TGF-ß induces a hypertrophic response in cultured ventricular cardiomyocytes and stimulates endogenous TGF-ß release (81). IL-6 and IL-6-like cytokines induce hypertrophic and anti-apoptotic pathways in cardiomyocytes through Akt activation (82).

Freshly isolated neonatal cardiomyocytes were used to determine whether PC12-conditioned media induced a greater effect at the single-cell level than cardiomyocytes treated with identical doses of NE alone. Our data strengthen the hypothesis that there exist secondary factors released by pheochromocytoma cells that alter the pathogenesis of cardiomyopathy beyond the response seen with catecholamines alone, at low levels increasing function of and strain on cardiomyocytes, and at higher levels hastening loss of function. While an overload of catecholamines may be sufficient for the pathogenesis of PICM, we suggest that these are not wholly responsible, and may even be unnecessary for the development of cardiomyopathy in patients; these findings may also begin to explain the development of PICM in clinically-silent and normo-adrenergic pheochromocytoma patients (43). We also validated a new approach for studying the complete effects of pheochromocytoma on cardiomyocyte and cardiac physiology.

Although the role of the cytoskeleton as a stabilizing factor of cellular structure and functional integrity is well established, the structural basis of cardiomyopathy and heart failure is still not completely understood (83). In recent years mutations in at least five genes have been identified as causes of dilated cardiomyopathy and its clinical manifestations, including the contractile apparatus proteins dystrophin (84), desmin (85, 86), and vinculin (87). Studies have also shown a strong association between elevated expression of microtubule proteins and altered cardiac contractility (88), in which increased β-tubulin levels increase cardiomyocyte viscosity and stiffness (89). Importantly, these contractile apparatus proteins are all also important biomarkers for structural cardiovascular disease: well-established pathways of cardiomyocyte

remodeling in the context of heart failure involve compensatory cytoskeletal remodeling via the up-regulation of β-tubulin, vinculin, dystrophin and desmin. Our data suggest that *in vitro* studies done to date using NE alone to approximate the entire pheochromocytoma secretome may mask its true effects on cardiomyocyte remodeling, as these conditions elicit dramatically different patterns of damage and response. Indeed, whereas at high doses NE-induced protein changes approximate heart failure, complete PC12-media induced reductions (uncharacteristic of heart failure) in β-tubulin, vinculin and desmin. Furthermore, our data indicates that PC12 cell secretions induce a greater frequency of contraction than equivalent doses of NE alone and that encapsulation of PC12 cells does not affect their ability to secrete bioactive factors. More importantly, our observations demonstrate a different pattern of remodeling in response to the entire spectrum of pheochromocytoma-secreted factors. Here we show high degrees of correlation between all four proteins with each of the others examined when incubated with pheochromocytoma-conditioned media (Table 2). In marked contrast, only one set of proteins, desmin-dystrophin, was correlated in the context of NE alone. These data reveal a coordinated remodeling response, masked in simplified NE-only models, that begins to offer mechanistic insight into the pathogenesis of PICM.

The protein cytoskeletal changes exhibited to a greater degree and in different patterns following PC12-conditioned media exposure than equivalent doses of NE alone corroborate the belief that pheochromocytomas secrete secondary factors that alter cardiac function in addition to and possibly independent of secreted catecholamines. Our cytoskeletal data do not indicate a mechanism of damage, but clearly demonstrate dose-dependent cardiomyocyte remodeling via mechanisms involved in cardiomyopathy

and other cardiotoxic events. Furthermore, the diverging cytoskeletal remodeling seen in DCM versus our model of PICM might begin to explain the diverging reversibility of DCM and PICM.

We hypothesized that just as NE and complete pheochromocytoma secretions have differential effects on cardiomyocyte physiology *in vitro*, so too do these factors elicit different responses at the myocardial level *in vivo*. Traditional pheochromocytoma models have been hindered by the use of free pheochromocytoma cells whose unregulated growth and catecholamine secretion induce accelerated development of cardiomyopathy in the context of NE levels (40-75x basal levels) not always seen clinically (18, 21). These models, while yielding insight into the role of catecholamines in PICM, fail to explain the progression of the disease in patients with no observed catecholamine elevation, in those with lower levels of catecholamines (65), and the reversibility of PICM seen in early-stage pheochromocytoma patients (42, 68-70, 90).

We employed agarose encapsulation of PC12 cells to eliminate the unpredictable cell growth and NE release kinetics observed in previous systems. This approach has been used to success in studying other cell types, including Chinese hamster ovary cells (76). In this study, we determined the optimal cell density per agarose bead to maximize nutrient and oxygen transport to embedded cells, while restricting cell growth. This strategy resulted in predictable and reproducible cell growth and NE release kinetics mirroring that of PC12 cells grown in two-dimensional culture systems, allowing for direct comparison to osmotic pump-delivered NE alone over the period of study. Furthermore, implantation of agarose-encapsulated PC12 cells demonstrated that the

cells continued to grow and thrive *in vivo* for a period of 28 days while releasing predictable and quantifiable levels of NE.

To isolate the effects of catecholamines alone from the total pheochromocytoma secretome, we developed biodegradable microspheres releasing norepinephrine in a time-controlled manner. The microspheres upon hydration began to degrade thereby releasing the encapsulated norepinephrine for a period of 18 days, with a stable secretion window of 16 days. DL-PLGA was chosen for the polymer based on its biologically inert degradation products, DL-PLGA undergoes non-enzymatic hydrolysis to lactic and glycolic acids, which are eventually metabolized to carbon dioxide and water. Polymers of this class are often considered a standard for drug delivery purposes and are therefore reasonable selections for polymeric materials for intraperitoneal drug delivery. Several issues were encountered during in vitro testing of the biodegradable microspheres. In order to deliver NE doses identical to the encapsulated pheochromocytoma cells, approximately 200 mg of 600 μm beads would need to be implanted. Kohane et. al. demonstrated that such doses resulted high incidence of polymeric residue and adhesions beginning at 2 weeks after injection (Figure 11). Moreover histological analysis has revealed chronic inflammation, with foreign body giant cells prominent with particles greater than 5 μm in diameter (91). The high proclivity of the fibrous encapsulation of implanted DL-PLGA microspheres and the propensity to illicit an immune reaction coupled to the short stable time frame of NE release resulted in the use of an alternative method for NE release. Mini osmotic pumps were therefore chosen based on their ease of use, regularity of use as biological delivery agents and implantation in the peritoneal cavity.

The differential impact of pheochromocytoma-secreted factors versus NE alone was demonstrated in the ability of implanted PC12 cells to induce a greater degree of cardiomyopathy than equivalent doses of NE alone *in vivo*. Pheochromocytomas not only induced a greater increase in heart weight, but did so in the presence of lower plasma NE concentrations than rats implanted with NE pumps. The increased effects of PC12 cells were further observed at the single-cell level as changes in cytoskeletal protein levels, similar in degree and direction of alteration to our *in vitro* observations. Pheochromocytoma cells induced significant decreases in desmin, β-tubulin, and vinculin expression, each to a greater degree than by NE alone. In rats implanted with pumps secreting identical doses of NE alone expression of these proteins was reduced to a lesser extent, except in the case of desmin, which was indistinguishable from controls. Moreover, alterations in these cytoskeletal protein levels exhibited high degrees of correlation with each other, indicating coordinated myocardial remodeling responses, similar to cardiomyocytes *in vitro* (Table 2). Together these data demonstrate that pheochromocytoma secretions induce dissimilar cardiac changes at both the single-cell and whole-heart level in comparison to equivalent doses of NE alone.

In our novel models, PC12-conditioned media induced greater chronotropic effects and altered patterns of cardiomyocyte remodeling than equivalent doses of NE alone, suggesting net-additive effects of PC12 paracrine and endocrine factors on contractility and toxicity. This, together with the observation that pheochromocytomas induce dose-dependent cytoskeletal derangements different from those seen in both NE

and organic and compensatory DCM, suggests a different pathologic process at play than seen in both the traditional model of clinical cardiomyopathy and the preferred basic approach of studying PICM *in vitro*. Our findings may yield a more physiologic model of PICM that may begin to explain disparities between clinical and bench models of this disease.

5 Pheochromocytoma-Induced Cardiomyopathy is Modulated by the Synergistic Effects of Cell-Secreted Factors

Abstract

Pheochromocytomas are rare tumors derived from the chromaffin cells of the adrenal medulla. While these tumors have long been postulated to induce hypertension and cardiomyopathy through the hypersecretion of catecholamines, catecholamines alone may not fully explain the profound myocardial remodeling induced by these tumors. We sought to determine whether changes in myocardial function in pheochromocytoma-induced cardiomyopathy result solely from catecholamines secretion or from multiple pheochromocytoma-derived factors. Isolated cardiomyocytes incubated with pheochromocytoma-conditioned growth media contracted at a higher frequency than cardiomyocytes incubated with norepinephrine only. Sprague-Dawley rats and Black-6 mice were implanted with agarose-encapsulated pheochromocytoma (PC12) cells, DOPA decarboxylase knock-out PC12 cells deficient in norepinephrine (PC12-KO), or norepinephrine-secreting pumps. PC12 cell implantation increased left ventricular dilation by 35±6 and 9.6±1.4%, and reduced left ventricular fractional shortening by 20±3 and 28±4%, in rats and mice compared to animals dosed only with norepinephrine. Elimination of norepinephrine secretion in PC12-KO cells induced neither cardiac dilation nor changes in fractional shortening compared to controls. Reintroduction of NE secretion via NE secreting pumps implanted alongside PC12-KO cells induced cardiac dilation and reduced fractional shortening similar to intact PC12

cells. Pheochromocytomas induce a greater degree of cardiomyopathy than equivalent doses of norepinephrine, suggesting pheochromocytoma-induced cardiomyopathy is not solely mediated by norepinephrine, rather pheochromocytoma secretory factors in combination with catecholamines act synergistically to induce greater cardiac damage than catecholamines alone.

5.1 Introduction

Pheochromocytomas are rare but devastating tumors arising from chromaffin cells of the adrenal medulla or extra-adrenal paraganglia. These tumors often induce alterations in myocardial structure and function, leading to eventual development of severe cardiomyopathy(60-64). Pheochromocytomas are characterized by hypersecretion of catecholamines, namely norepinephrine (NE) and epinephrine, which are most often hypothesized to be the primary cause of tumor-induced alterations in cardiac function. Excessive adrenergic stimulation can induce and exacerbate cardiovascular disease(92-94). Exogenous epinephrine(27, 28) and norepinephrine (29, 30) are cardiotoxic in a dose-dependent fashion(17, 95). Cardiomyocyte viability decreases as a function of norepinephrine concentration(37) mediated by β-adrenergic receptor (βAR) stimulation, increased cAMP, and calcium influx(37). Selective stimulation of βARs mimics NE cardiotoxicity, and βAR blockade significantly attenuates these toxic effects(96). Infusion of NE increases systolic blood pressure (SBP), down-regulates βAR, and alters LV contractility. LV hypertrophy is characterized by multifocal mixed inflammatory infiltrates, acute myocyte degeneration(41, 95), and increased interstitial fibrosis(97-99).

However, it is still unclear whether catecholamine excess alone can explain the severity of cardiomyopathy with pheochromocytoma and heart failure in the absence of blood pressure effects. Only one-third of patients with these tumors are persistently hypertensive and onset of cardiomyopathy does not correlate with blood pressure or circulating catecholamine(46). Previous experiments with pheochromocytoma implants did not control cell growth and consequently NE secretions were excessively high, nor

did they directly compare pheochromocytoma effects to equivalent effects of NE alone(18, 22, 95). The lack of dose control makes direct comparison of cell and drug models problematic. It may be that these tumors secrete other factors that exacerbate catecholamine-induced damage or are cardiotoxic themselves(18, 26). To determine the factors secreted by pheochromocytoma cells responsible for cardiomyopathy induction at low levels of NE, the secretion of NE by pheochromocytoma cells must be replicated *in vivo* at a concentration and rate equal to that of pheochromocytoma-bearing animals. To investigate the development of dilated cardiomyopathy in the presence of a pheochromocytoma, we engineered a novel polymeric encapsulation system enabling the implantation of a pheochromocytoma cell line into a murine model, allowing for the control of tumor cell growth and subsequent factor secretion. The effects of pheochromocytoma cells on cardiac and cellular function and remodeling were compared to the effects of NE alone. Our successful development of a new animal model of pheochromocytoma-induced cardiomyopathy (PICM) allowed us to demonstrate differential effects of, and responses to, complete pheochromocytoma secretions versus catecholamines, yielding new insight into the etiology, pathogenesis, and approaches for treating PICM.

5.2 Methods

5.2.1 Cell Culture and Encapsulation

Rat pheochromocytoma cells (PC12, ATCC, VA) were maintained in F12K media (ATCC) with 10% horse serum (Hyclone, Logan, UT), 5% FBS (Hyclone) and 100 units/ml penicillin/streptomyocin (Invitrogen, CA)(19, 25). Cells were grown at 37°C and 5% CO_2, scraped and re-suspended in a preheated solution of 2.5% (w/w) agarose (Sigma–Aldrich, Type VII, MO) in 0.9% NaCl. The mixture was drawn into an Eppendorf Repeater Pipette with a 0.5 mL Combitip (VWR, MO) and 10 µL aliquots sheared into mineral oil (~600 mL) forming cell-encapsulating agarose beads as described(76). The beads were separated using a 1,000µm pore size mesh (Small Parts, FL) and washed with PBS. Cell number rose from 10^4 to $1.8*10^4$ cells per bead over 21 days and following growth kinetics of PC12 cells on tissue culture polystyrene plates. Each bead secreted 460 pg/day of norepinephrine by ELISA. Dopamine levels in PC12 cells were undetectable(78), as were epinephrine levels given the low or non-existent expression of phenylethanolamine-N-methyltransferase, the enzyme responsible for converting norepinephrine to epinephrine(49). The lack of epinephrine or dopamine secretion makes these cells then an ideal side-by-side comparison to the NE-secreting pumps.

5.2.2 Cardiomyocyte Contractility

Cardiomyocytes were obtained from 2-day-old neonatal Sprague-Dawley rats (Taconic). Cardiac ventricles were minced, incubated in trypsin (0.6 mg/mL in HBSS) for 16 hrs at 4°C and digested with collagenase type II (Sigma–Aldrich), 1 mg/mL. Cells were re-suspended in DMEM supplemented with 10% FBS, 25 mM HEPES and

penicillin [100 U/mL]). Each ventricle yielded ~ 6 x10^6 cells with viability between 88% and 94%. Myocytes were plated on 60 mm culture dishes and incubated with varying concentrations of control media, NE media, or PC12-conditioned media for 20 minutes. PC12 media was collected from separate dishes containing varying numbers of beads, the media was assayed for NE and matched with newly prepared NE media. Contractility was recorded in a temperature-controlled chamber mounted with a digital video camera (Olympus, DP70, NY). Cardiomyocyte contractility was quantified with MatLab (Mathworks, MA). All *in vitro* contractile studies were performed at constant temperature and CO_2 to reduce environmental impact on contractile function.

5.2.3 Transfection of DOPA decarboxylase Short Hairpin RNA (shRNA)

Phoenix cells (Orbigen, CA) were transfected with a single DOPA decarboxylase shRNA construct (Origene, MD) and were selected for 3 - 4 weeks in 2 μg/ml of puromycin to generate stably transfected, retrovirus-producing cells. Constructs used for shRNA were GGTGTATGGCTGCACATTGATGCTGCATA. PC12 cells were exposed to retrovirus expressing DOPA decarboxylase shRNA or empty vector in the presence of 0.5 μg/ml polybrene (Sigma) for 4 - 6 hours. The media was replaced with media containing retrovirus and the transfectants were incubated overnight. Transfected cells were then selected with 1 μg/ml puromycin for 4-5 weeks and used in experiments.

5.2.4 Animal Experiments

Female Sprague-Dawley Rats (8 weeks old, 250 g) and female Black-6 mice (7-8 weeks old, 15-20 g) were obtained from Taconic. All animal studies were performed in

accordance with protocols approved by the MIT Institutional Animal Care and Use Committee (IACUC) and Harvard Medical School's IACUC and with the Guide for the Care and Use of Laboratory Animals published by the US National Institutes of Health (NIH Publication No. 85-23, revised 1996). Osmotic pumps (Alzet, Model 2004 (rats) and Model 1004 (mice), CA) or agarose-encapsulated PC12 cells were implanted in the retro-peritoneal cavity, mimicking the spatial release of pheochromocytoma cells. A total of 20 agarose-encapsulated PC12 or PC12-KO beads were implanted. The 9.2 ng/day NE secretion rate of the 20 agarose-PC12 beads was matched with osmotic pumps (Alzet) delivering 0.25 μL/hr (rats) and 0.11 μL/hr (mice) loaded with 9.06 and 21 μM solution of NE in acidic saline (0.1mg/mL ascorbic acid in saline) for rats and mice, respectively. The ascorbic acid solution retards catecholamine oxidation. For the NE rescue experiments PC12-KO cells were implanted alongside NE secreting pumps identical to the NE alone experiments.

Catecholamine levels were tracked through weekly blood draws via the retro-orbital plexus and quantified by ELISA (Rocky Mountain Diagnostics). Control animals received osmotic pumps loaded with acidic saline carrier solution alone. Animals implanted with empty agarose beads and non-surgical, non-implanted animals had statistically identical cardiac dimensions and mRNA levels.

5.2.5 Echocardiographic and Hemodynamic Measurements

Echocardiography of anesthetized rats (pentobarbital 30 mg/kg IP) was performed at the 56-day endpoint with a linear array probe (Visual Sonics, RMV710B, Toronto, Canada) and a Visual Sonics Vevo 770. Cardiac dimensions were obtained from M-mode tracings using measurements averaged from three separate cardiac cycles by an echocardiographer blinded to the rat's genotype. Arterial pressure was recorded by inserting a pressure-conductance catheter (Millar Instruments, SPR-878, TX) into the LV via the right internal carotid artery. The catheter was connected to a pressure-conductance unit (Millar Instruments, MPVS-400) and waveforms were recorded using ChartV5 software (AD Instruments, CO). Data were analyzed with Millar PVAN 3.4 (Millar Instruments). Four randomly selected rats from each group were chosen for analysis.

Transthoracic echocardiography was performed in anesthetized mice (2%isoflurane) using a 12-MHz probe and a Sonos 5500 ultrasonograph (Hewlett-Packard, MA). Left ventricular parameters and heart rates were obtained from M-mode interrogation in a short-axis view, averaged from three separate cardiac cycles at heart rates greater than 400 beats/minute. The echocardiographer was blinded to mice genotypes. Cardiac contractile function was represented by the parameter LV fractional shortening (percentage), calculated as [(LV diastolic diameter – LV systolic diameter)/LV diastolic diameter] x 100.

5.2.6 Histological Analyses

Animals were euthanized, hearts excised, rinsed in PBS, weighed, then pressure perfused (100 mmHg) with PBS for 5 minutes followed by 10% neutral buffered formalin (NBF) until visibly firm and pale. The hearts were placed in 10% NBF overnight, processed, paraffin fixed (Polysciences Inc., PA), and serial coronal sections cut and stained with hematoxylin and eosin (Sigma–Aldrich) and Gomori's Trichrome (American HistoLabs Inc., MD). A pathologist blinded to the treatment groups graded the tissues. TUNEL assay was performed with an apoptosis kit (Millipore, MA) according to manufacturer's instructions. Six images per heart were acquired on Leica microscope. Results were expressed as the number of apoptotic nuclei per total nuclei per image field.

5.2.7 RNA Preparation and RT-PCR

Excised hearts were perfused with PBS and a biopsy (8x 8mm) taken. Total RNA was isolated with the use of Qiashredder and RNeasy spin columns (Qiagen, CA). cDNA was synthesized using Taqman RT-PCR kit (Applied Biosystems, CA). Specific primers were designed using Primer3(77). Real-time polymerase chain reaction (PCR) was performed with an Opticon Real Time PCR Machine (Biorad, CA) using SYBR Green PCR Master Mix Reagent Kit (Applied Biosystems). All samples (n=5 per group) were measured in triplicate and the expression level was normalized to GAPDH expression.

5.3 Results

5.3.1 Cardiomyocyte Contractility

Freshly isolated neonatal cardiomyocytes were used to determine whether PC12- conditioned media induced a greater effect at the single cell level than cardiomyocytes dosed with identical concentrations of only NE. PC12-conditioned media caused cardiomyocytes to contract at a higher frequency than those incubated with identical NE doses and with nearly two-fold greater contractility at 0.07 nM ($p<0.01$) (Figure 12). The increased beating frequency induced by PC12-conditioned media compared to identical doses of NE occurred in a dose-dependent fashion.

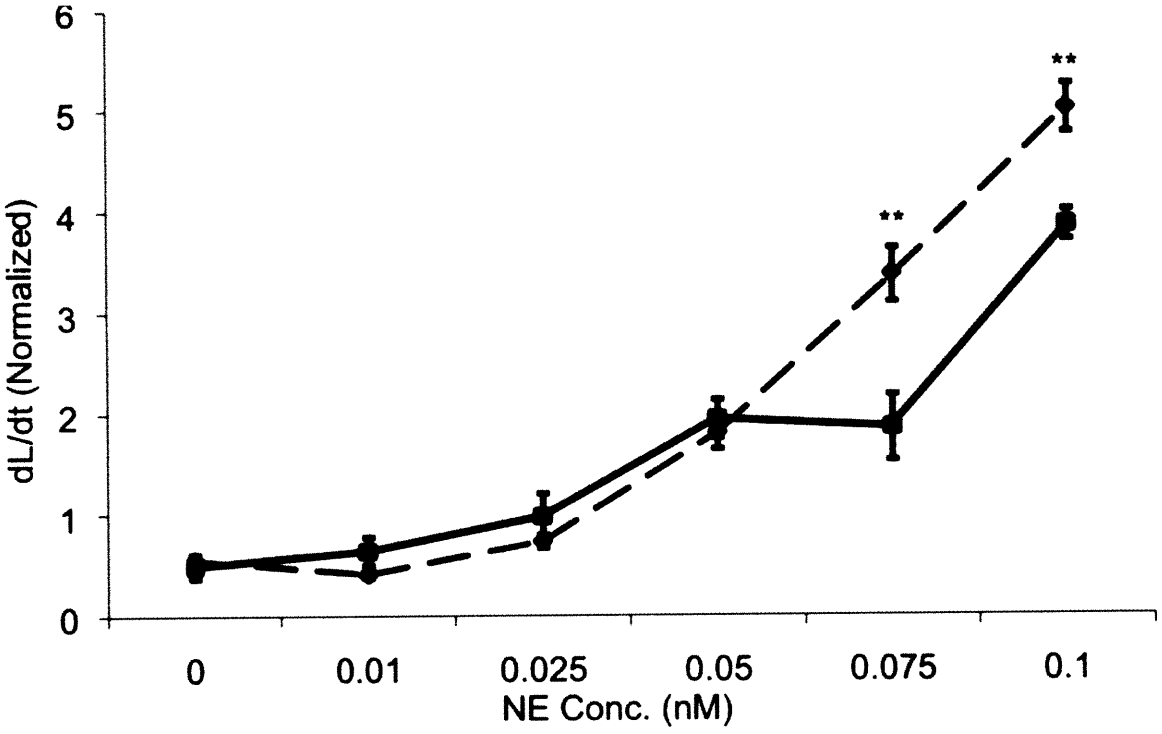

Figure 12. Conditioned media from PC12 cells (dashed line) induces a greater change on cardiomyocyte contractility than norepinephrine media (solid line). The data at each time point is the mean ± SE of n= 4 separate culture plates. **P < 0.01.

5.3.2 Rat and Mouse Models, Cardiac Morphology, and Function

Experiments were performed in two species to verify the nature of the effects. NE secretion in pheochromocytoma-implanted (Pheo) animals was matched with the implantation of NE secreting pumps (Figure 13). Implanted pumps and PC12 cells in rats raised NE plasma value by 0.4 and 0.3 ng/mL, respectively. Implanted pumps, PC12 cells, PC12-KO cells (Pheo-KO), and PC12-KO cells plus NE pumps in mice raised NE plasma values by 4, 3, 0.7, and 4.5 ng/mL, respectively. To ensure the cardiac pathology observed was not a result of the host-PC12 cell interaction instead of PC12 secreted factors, empty agarose beads were implanted and their effects on cardiac pathology were compared to control rats. The heart weight normalized to body weight of rats implanted with empty agarose beads (6.0±0.5 μg/g) was statistically identical to control rats (6.3±0.4 μg/g). There was no detectable histological difference in the cellular and tissue response, indicating that host-cell interactions would not be a factor cardiomyopathy development.

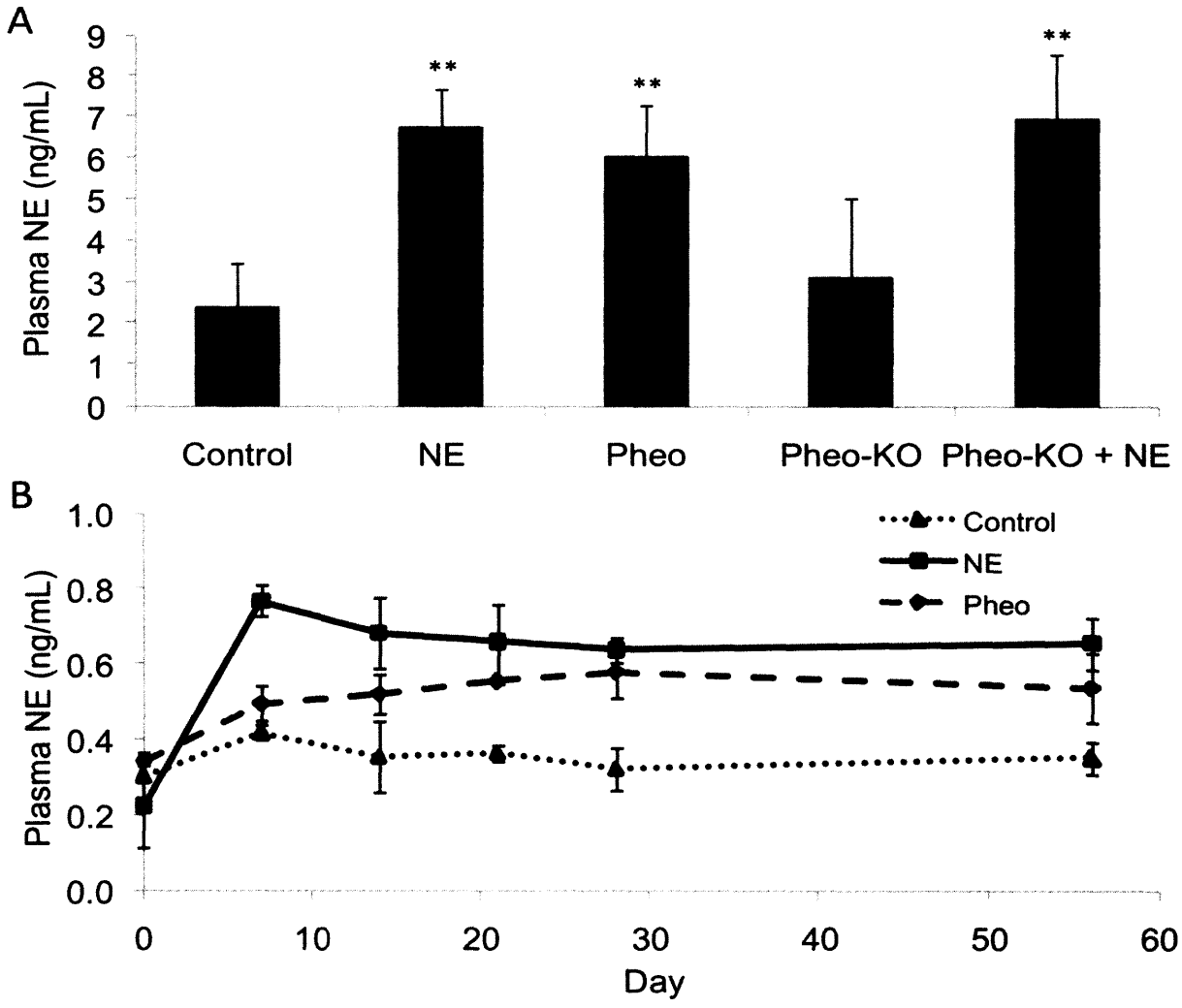

Figure 13. Norepinephrine levels secreted by pheochromocytoma cells were matched via the implantation of osmotic pumps. (A) The plasma NE levels were statistically equal in mice implanted with NE pumps and PC12cells and elevated in comparison to control and PC12-KO mice. Control and PC12-KO mice NE levels were statistically indistinguishable. (n=5 mice per group, n=4 control mice). (B) Plasma NE levels were statistically equal in rats implanted with NE pumps, PC12 and PC12-KO cells + NE pumps cells and elevated in comparison to control rats. (n=5 rats per group). *$P < 0.05$, **$P < 0.01$ versus controls.

Cardiac dilation was more pronounced in Pheo rats and mice ($p<0.01$ vs. control, $p<0.01$ vs. NE) compared to NE rats and mice (Figure 15,A). The hearts of Pheo rats were 47% larger than controls ($p<0.01$) and NE rats ($p<0.01$), the latter statistically indistinguishable from controls (Table 3). Similarly, Pheo mice developed a 22% greater degree of dilation over NE mice ($p<0.01$), 17% dilation over Pheo-KO mice and 61% greater than controls ($p<0.01$). Furthermore Pheo mice experienced a greater loss of cardiac function, evident in the 10.8±1.9% ($p<0.01$ vs. control, $p<0.05$ vs. NE) decrease in fractional shortening (FS) compared to NE mice that experienced a 6.3±2.9% ($p<0.01$) decrease in FS. These changes occurred despite the absence of significant increases in the SBP or heart rates, and both were statistically indistinguishable from Pheo, Pheo-KO and NE mice (Figure 15, B-C). Of note, Pheo-KO mice did exhibit slight increase in cardiac dilation but no discernible loss of FS compared to controls (Table 4). When NE is reintroduced into the PC12-KO secretome by NE secreting pumps the mice experience a 12% increase in cardiac dilation and a 20% loss of cardiac function. The degree of loss of cardiac function is similar to that of intact PC12 cells indicating the catecholamines alone are necessary to induce the full cardiac effects of pheochromocytomas but not sufficient on their own (Figure 11, A). PC12-KO cells implanted in conjunction with NE secreting pumps raised circulating plasma NE levels (Figure 13, A) to those experienced with intact PC12 cells with no discernible hemodynamic effects (Figure 13, B-C).

Left ventricular end-systolic volume scaled linearly with norepinephrine levels (R^2=0.916, $p<0.0001$) in control, pheo and pheo-KO mice but not in NE pump animals whose catecholamine levels were all at the upper limit and without correlative effect. Histologic analyses of cardiac tissue showed little microscopic difference between Pheo, NE, Pheo-KO and control animals (Figure 16). TUNEL-positive apoptotic cells were identified in greatest density in Pheo animals (1.53±0.90 apoptotic nuclei/total nuclei, p=0.25 vs. NE, p=0.10 vs. control), intermediate density in NE animals (0.97±0.60 apoptotic nuclei/total nuclei, p=0.79 vs. control), and lowest density in control animals (0.86±0.60 apoptotic nuclei/total nuclei) (Figure 14).

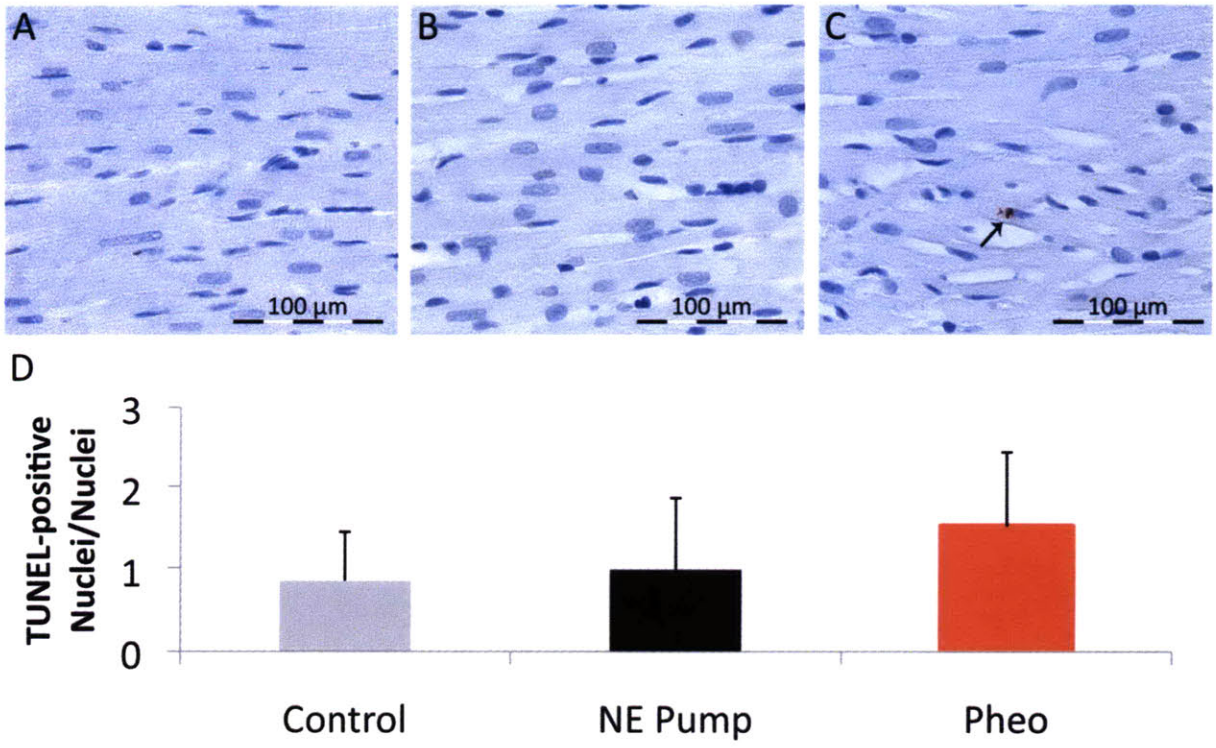

Figure 14. Implanted pheochromocytoma cells induced greater cardiomyocyte apoptosis than NE implanted and control rats. Representative TUNEL stained LV tissue sections for Pheo (A), NE (B), and Control (C) mice. Arrow in (C) indicates a apoptotic cell. (D) Pheo implanted mice exhibited greater density of TUNEL-positive nuclei per total nuclei. The number of TUNEL-positive nuclei between experimental groups and controls was not statistically significant.

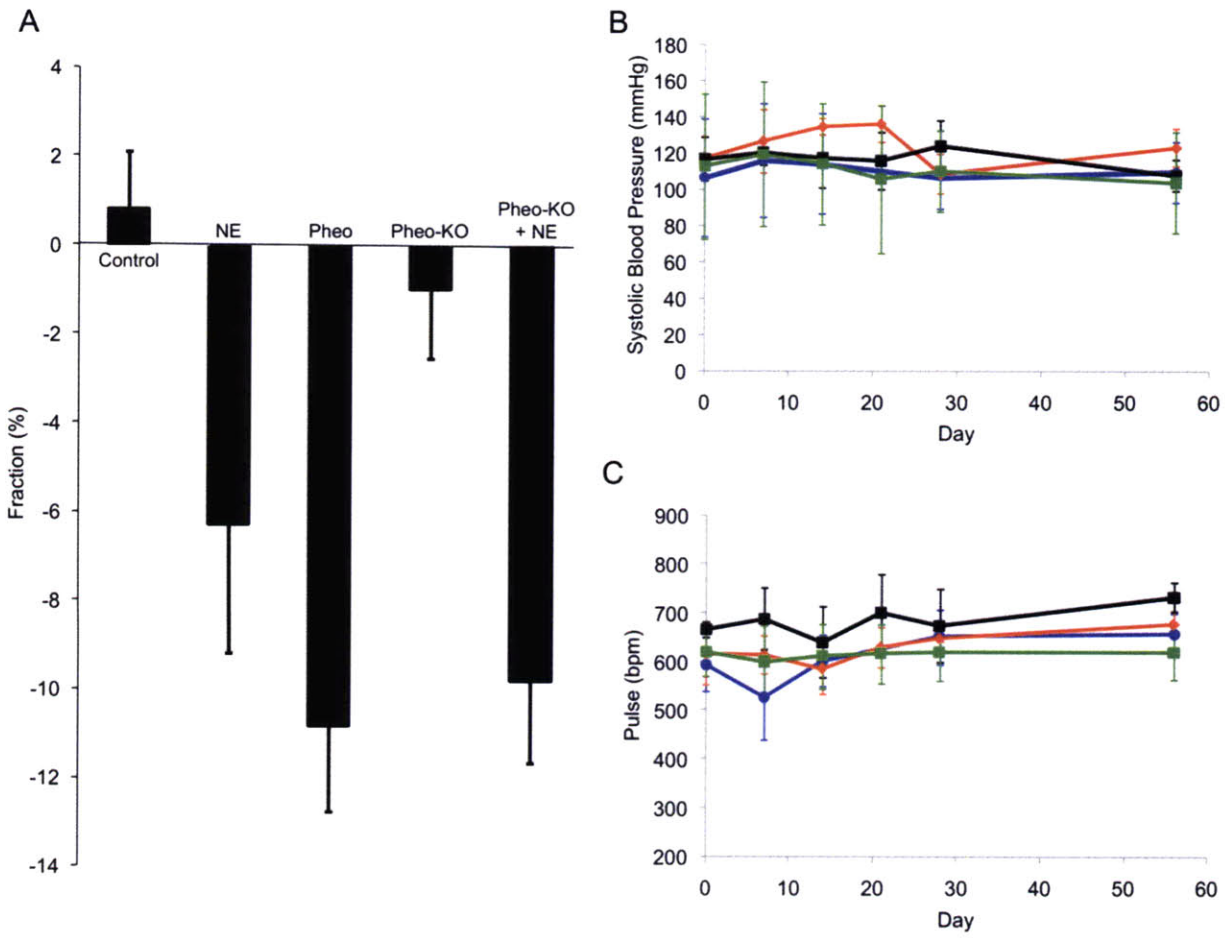

Figure 15. Implanted pheochromocytoma cells induce greater cardiac dysfunction than equivalent doses of NE alone. (A) Change in fractional shortening (white) and ejection fraction (black) from Day 0 to Day 56 for Control, NE, Pheo, Pheo-KO and Pheo-KO + NE mice. (B) Low doses of NE secreted by the implanted NE pumps (black), PC12 cells (red), PC12-KO (blue), and PC12-KO + NE cells (green) had no effect on SBP. (C) The heart rates of mice implanted with NE pumps (black), PC12 cells (red), PC12-KO (blue), and PC12-KO + NE cells (green) were indistinguishable. (n=5 per group, n=4 control mice).

Table 3. Cardiac Morphology and Function of Control, NE and Pheo rats.

Characteristic	Control	NE	Pheo
No. of rats	7	8	7
Age, weeks	10±2	10±2	10±2
HW:TL (g:cm)	0.17±0.04	0.19±0.02†	0.25±0.02**,††
HR (bpm)	317±15	360±45	362±19
SBP (mmHg)	104±17	84±18	94±30
LVWT, mm	1.16±0.12	1.18±0.16	1.00±0.19
LVEDD, mm	5.5±0.1	6.0±0.6††	8.1±0.3**,††
LVESD, mm	2.4±0.6	3.4±0.6††	5.3±0.3**,††
FS, %	49±4	43±2	34±3*,††
EF (%)	39±6	36±4	27±4††

SBP, systolic blood pressure; LVWT, LV wall thickness at end diastole; LVEDD, LV end diastolic diameter; LVESD, LV end systolic diameter; FS, fractional shortening; EF, ejection fraction. Values are means ± SD. *P < 0.05, **P < 0.01 versus NE rats; †P < 0.05, ††P < 0.01 versus controls.

Table 4. Cardiac Morphology and Function of Control, NE, Pheo and Pheo-KO mice.

Characteristic	Control	NE	Pheo	Pheo-KO	Pheo-KO + NE
No. Mice	4	6	6	6	6
Age (weeks)	7±2	7±2	7±2	7±2	5±2
ΔLVWT (mm)	-0.03±0.01	-0.13±0.03†	-0.09±0.03	-0.04±0.02	-0.02±0.03
ΔLVEDD (mm)	-0.03±0.01	0.24±0.09†	0.34±0.04††	0.26±0.08*†	0.16±0.06*†
ΔLVESD (mm)	-0.01±0.01	0.43±0.11††	0.63±0.07*,††	0.2±0.07†	0.25±0.04††
ΔFS (%)	-1.2±0.3	-6.3±2.9	-10.8±1.9*,††	-1.0±1.5	-9.8±1.8††
ΔEF (%)	3.4±0.6	-8.8±3.8	-21.5±4.2	-1.6±1.9	-19.2±4.0

ΔLVWT, change in LV wall thickness at end diastole; ΔLVEDD, change in LV end diastolic diameter; ΔLVESD, change in LV end systolic diameter; ΔFS, change in fractional shortening; ΔEF, change in ejection fraction. Values are means ± SD. *P < 0.05, **P < 0.01 versus NE rats; †P < 0.05, ††P < 0.01 versus controls.

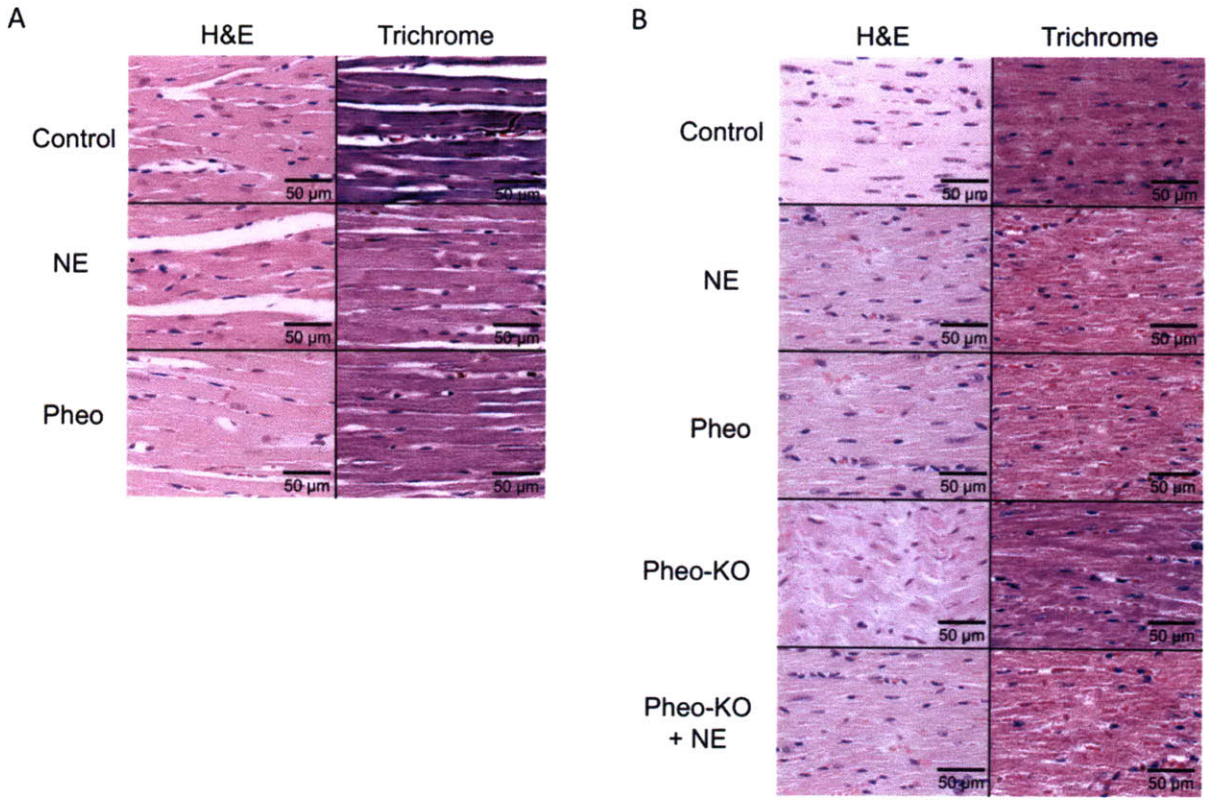

Figure 16. Low doses of NE released by pheochromocytoma cells and NE secreting pumps result in dimensional changes in cardiac tissue without attaining irreversible damage at subcellular level. Representative images from the hearts of rats (A) and mice (B) stained with Hematoxylin and Eosin and Gomori's Trichrome. Histopathology of NE, Pheo, Pheo-KO, and Pheo-KO + NE animals exhibited no myocyte disarray or fibrosis. All images taken at 40x magnification. (n = 5 animals per group, n = 4 control animals per group).

Cardiac function was further characterized by left ventricular (LV) catheterization 56 days after cell implantation or NE infusion. At the doses tested, NE increased myocardial function above control, with a steeper slope of the end-systolic pressure-volume relationship (ESPVR) ($p<0.05$), decreased end diastolic pressure ($p<0.05$), and a higher maximum ventricular elastance ($p<0.01$) (Figure 17, D-F). In contrast, at the same doses of NE released, pheochromocytoma cells reduced all indices of cardiac function. There was a 73% reduction in the slope of the ESPVR ($p<0.01$ vs. NE rats, $p<0.01$ vs. control), a 24% decrease in end diastolic pressure ($p>0.05$ vs. NE rats, $p<0.01$ vs. controls), and a 70% decrease in ventricular elastance ($p=0.017$ vs. NE rats, $p< 0.01$ vs. controls) (Table 5). The decreased ESPVR slope reflects a decrease in the heart's inotropic capabilities. To maintain stroke volume under these circumstances, the ventricle will often operate at higher volumes in a process of compensatory dilation. This mechanism is further validated by the 96% and 36% increase in stroke volume for Pheo rats over controls and NE rats, respectively.

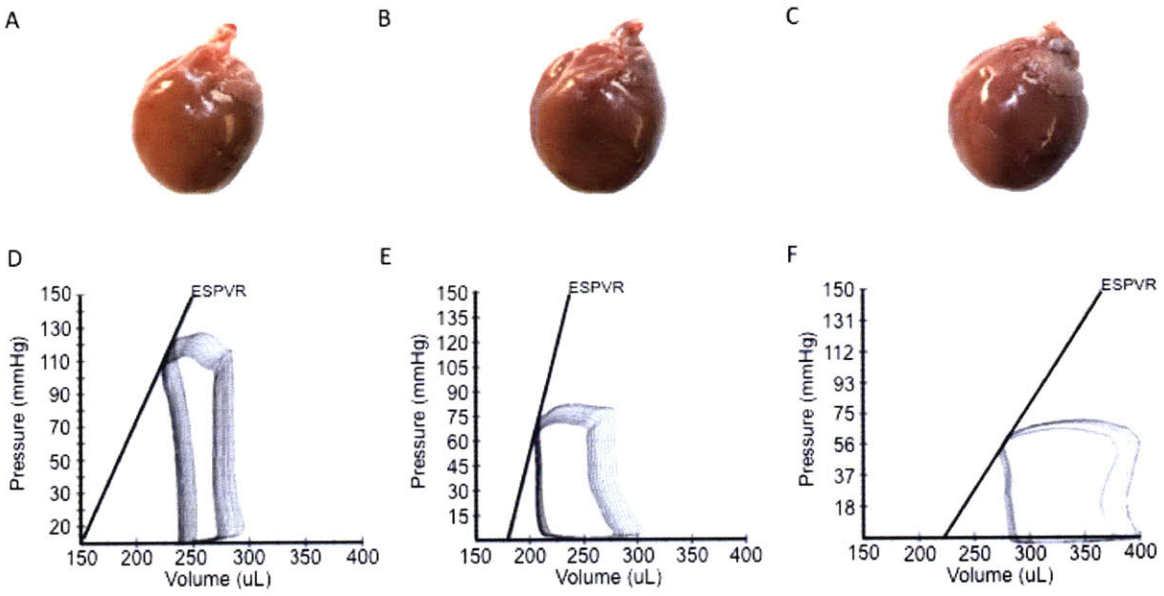

Figure 17. Rats implanted with pheochromocytoma cells experience greater cardiac dysfunction than equivalent doses of NE alone. Representative images of the hearts of Control (A), NE pump (B) and Pheo (C) Rats. (D-F) Representative left ventricular pressure-volume loops obtained at the 56-day endpoint for Control (D), NE (E) and Pheo (F) rats. End-systolic pressure-volume relationship (ESPVR) during preload reduction is indicated by the black line (n=5 rats per group).

Table 5. Hemodynamic Measurements of Control, NE and Pheo rats.

Characteristic	Control	NE	Pheo
ESPVR Slope (mmHg/L)	1.49±0.16	1.04±0.33	2.58±0.20**,††
Stroke Volume (uL)	53.3±1.4	76.4±6.0††	104.3±7.6**,††
End Diastolic Pressure (mmHg)	4.51 ±0.14	3.47±0.61†	3.41±0.25††
End Diastolic Volume (uL)	275.5±3.5	284.3±3.4††	392.2±28.3**,††
Elastance (mmHg/uL)	2.19±0.32	0.954±0.18††	0.64±0.10**,††

Values are means ± SD. (n = 5 for all groups). *p<0.05, **p<0.01 versus NE rats;

†p<0.05, ††p<0.01 versus controls.

NE levels were detectable in all animals and even the lowest catecholamine doses correlated with LV dilation. This was the case in cell implants and controls, but not in NE pump animals nor PC12-KO animals with NE pumps. It is possible that the circulating NE levels reflect the degree of heart failure as in humans(100, 101) and correlate with the left ventricular end systolic volume (LVEDV) not fractional shortening or ejection fraction (Figure 18). Animals implanted with NE pumps induced a range of cardiomyopathic effects without a direct correlation to LVEDV. In contrast, a correlation was observed in animals with encapsulated PC12-KO cells, even at the very low doses of detectable NE levels. In all, the implantation of PC12-KO cells resulted in no elevation of plasma NE levels or changes in fractional shortening or ejection fraction.

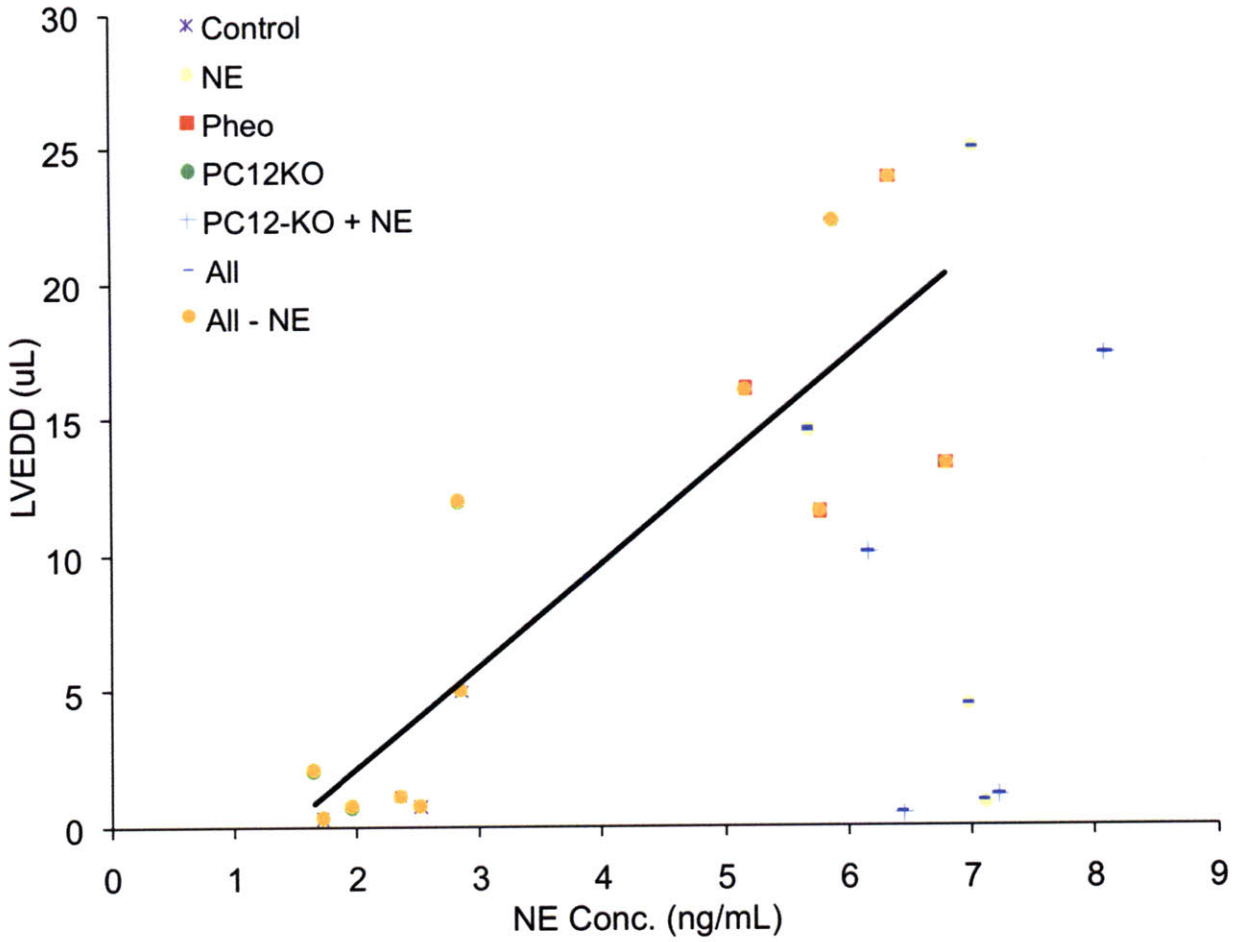

Figure 18. NE Secreted by PC12 and PC12-KO cells strongly correlates to left ventricular end diastolic diameter (LVEDD). NE secreted by NE pumps demonstrates no correlation to LVEDD.

5.3.3 Myocardial Gene Expression

Cardiac extracellular matrix biomolecules play a central role in maladaptive myocardial remodeling and cardiac decompensation. Clinical studies over the past decade have shown increased levels of CC chemokine ligand 2 (CCL2, MCP-1), matrix metalloproteinase 3 (MMP3), collagen-1 and decreased levels of tissue inhibitor of matrix metalloproteinases 3 (TIMP3) to be associated with cardiovascular disease and cardiac dysfunction (24, 102, 103). Pheo-implants raised MMP3 ($p<0.01$), collagen-1 ($p<0.05$), CCL2 ($p < 0.01$) and reduced TIMP3 ($p <0.01$) mRNA levels compared to NE rats (Figure 19). BNP mRNA levels were elevated 2.8±0.2 fold above control animals 28 days after implantation and remained elevated for the duration of the experiment. It took twice as long for NE rats to exhibit the same level of elevation. Levels of mRNA were identical to controls (100±20% over controls) at 28 days and became elevated (290±50% over controls) only at 56 days. These statistically significant changes highlight the ability of pheochromocytomas to induce cardiac pathology with accelerated kinetics versus NE alone. The changes in gene expression values bear a strong correlation to the heart's morphological and functional changes as diagnosed echocardiographically. Specifically, increasing CCL2 levels correlate strongly with increasing left ventricular end diastolic diameter (LVEDD) ($R^2= 0.92$, $p<0.0001$) and decreasing fractional shortening ($R^2 = -0.84$, $p=0.000$). Similarly, increases in MMP3 and collagen correlate with increasing LVEDD ($R^2= 0.86$, $p<0.0001$ for MMP3 and $R^2= 0.73$, $p=0.003$ for collagen), with increases in collagen highly correlative with decreases

in fractional shortening (R^2 = -0.94, $p<0.0001$). TIMP3 mRNA levels further correlate with LVEDD (R^2 = -0.81, $p<0.0001$) and fractional shortening (R^2 = 0.66, $p=0.010$).

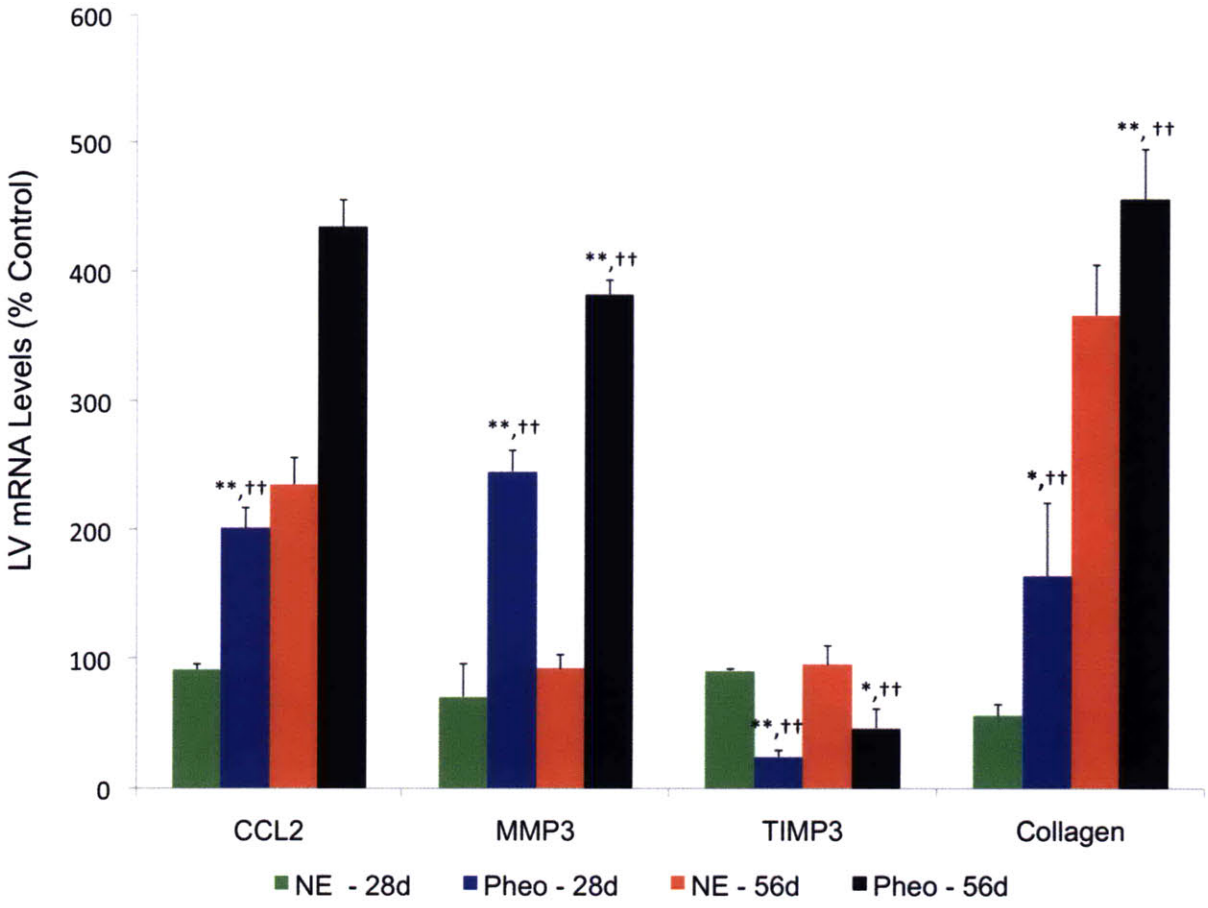

Figure 19. Rats implanted with pheochromocytoma cells increase mRNA levels of cardiac dysfunction associated proteins. Quantification of left ventricular mRNA levels for Pheo and NE rats at 28- and 56-day. The mRNA levels were normalized to percent controls. CCL2, MMP3 and collagen mRNA levels were upregulated to a greater degree in rats implanted with pheochromocytomas than those implanted with NE pumps. TIMP3 levels were down regulated to a greater degree in pheo rats than NE rats (n=5 rats per group). *P < 0.05, **P < 0.01 versus NE rats; †P < 0.05, ††P < 0.01 versus controls.

5.4 Discussion

While catecholamines may dominate the cardiotoxic effects of late-stage pheochromocytomas, the secretion of low levels of catecholamines during early tumor development is insufficient to induce hemodynamic effects. Indeed, only 29% of all pheochromocytoma patients are persistently hypertensive, and only another 30% demonstrate episodic hypertension(61, 104). Previous research has attributed the cardiotoxicity of pheochromocytomas to catecholamines but has not addressed whether other tumor secreted factors act to induce myocardial remodeling(18). Here we employ agarose-encapsulation of PC12 cells that enables quantifiable and reproducible control of cell growth and NE release allowing for the matched secretion of NE by the PC12-agarose beads with implanted norepinephrine releasing osmotic pumps. We focused on the impact of low-grade, low-NE secreting tumors to separate the effects of non-catecholamine secretory products of early-stage pheochromocytomas from those of late-stage tumors with NE hypersecretion.

In-vitro, pheochromocytoma cell conditioned media induced more frequent cardiomyocyte contractions than NE alone suggesting that catecholamines are not solely responsible for the effects of pheochromocytomas on cardiomyocyte physiology. The increased effects elicited by intact pheochromocytoma secretions indicate that the intact secretory products of pheochromocytoma including norepinephrine are more potent than the sum of the individual factors. It may very well be that pheochromocytomas either secrete secondary factors that have a direct effect on the cardiomyocytes or that the ability of pheochromocytomas to induce cardiac pathology is dependent upon the synergistic action of the entire secretory cocktail.

Animals implanted with PC12 cells exhibited far greater structural and functional impairment than animals with NE implants, all without changes in blood pressure or heart rate. In these similar hemodynamic domains, only pheochromocytoma cells induced significant cardiomyopathy in mice and rats. These changes closely mimic the human consequences of these tumors, as LV chamber size was enlarged, fractional shortening was reduced, and hemodynamic function altered, all to a far greater degree than with equivalent NE doses. These effects were absent with the elimination of NE secretion from PC12-KO cells, whose implantation failed to induce a cardiomyopathic state. The reintroduction of norepinephrine into the pheochromocytoma knock-out cell secretome via NE secreting pumps induced a cardiomyopathic state equivalent to intact pheochromocytoma cells. The induction of cardiomyopathy therefore likely results from the confluence of pheochromocytoma-secreted factors, rather than from a single factor alone. Though NE is necessary to induce cardiomyopathy, it is not sufficient to explain the full force of the effects of pheochromocytoma on the heart.

The altered balance of the cytoskeletal proteins, MMP3, TIMP3, and collagen, creates maladaptive myocardial remodeling that mediates the transition from compensated to decompensated heart failure(24, 102, 103, 105). MMP3 elevation and reduction in its inhibitor, TIMP3, exacerbates ventricular dilation by disintegrating the collagen network(102). High dose NE infusion increased myocardial collagen, myocyte diameter, and fibrosis with elevated TIMP3 and MMP3 mRNA levels(41). In line with these observations, collagen and MMP3 mRNA levels were significantly increased and TIMP3 levels decreased in pheochromocytoma-implanted animals. The hearts of

animals exposed to low doses of NE alone expressed minimal alterations in collagen, cardiac function, MMP3 levels, and TIMP3 levels. Other inflammatory mediators involved in the pathogenesis and progression of heart failure followed suit to provide further mechanistic insight. CCL2 mediates myocardial remodeling by promoting the attraction and invasion of activated leukocytes into damaged or inflamed tissue. Circulating CCL2 levels rise significantly in advanced dilated cardiomyopathy, congestive heart failure, and ischemic reperfusion injury(106, 107). Similarly, CCL2 levels increased significantly in Pheo implanted rats at day 28 and continued to rise at day 56. In contrast, NE rats expressed normal levels of CCL2 at day 28 compared to controls, with levels only rising at 56 days. Our data demonstrating that CCL2 mRNA levels were upregulated to a greater extent in Pheo versus NE rats coincides with the changes seen in a variety of clinical structural pathologies(35).

Current data indicate that cardiac markers of cytoskeletal remodeling, injury, and fibrosis are upregulated prior to their physical manifestation and are evident sooner in Pheo animals than NE animals. These subcellular effects occur prior to the onset of frank cardiomyopathy. The rapid onset of these subcellular effects, evident after 28 days of implantation, and sooner than the onset of cardiomyopathy, evident at 56 days, further highlights the severity of this disease and urgent need for diagnosis and treatment. Moreover, these data indicate that the cardiomyopathic symptoms evident at day 56 may be a secondary result of drastic cardiomyocyte remodeling and loss of function. The differences between experimental groups highlight the greater synergistic effects of pheochromocytoma secretory products and their ability to induce a more severe cardiac pathology. It therefore becomes necessary to develop more accurate

screening tools to identify pheochromocytomas and reduce the drastic subcellular effects of pheochromocytomas.

Taken together, our findings suggest that pheochromocytoma tumor cells in combination with their catecholamines act synergistically to induce greater cardiac damage than catecholamines alone. Numerous factors secreted by pheochromocytoma cells can directly or indirectly alter heart function(108, 109). Our works suggests that it is the confluence of these factors that enable the synergistic induction of myocardial injury. The implications of our work lie not only in a better understanding of pheochromocytomas and their secretory products but also in the differences between cell-secreted substances and their exogenous analogues in isolation. Given that secondary factors are sufficient to induce PICM in early-stage patients, these data further highlight the need for understanding the fundamental development of early pathology for the purpose of basic insight into cardiomyopathies, and developing novel therapeutic approaches.

6 The Effects of the Gravid State on the Development of Pheochromocytoma-Induced Cardiomyopathy

6.1 Introduction

A mechanism of special interest is the increased proclivity for dilated cardiomyopathy in the presence of pheochromocytomas in gravid females. Pheochromocytomas have been identified in 1 in 40,000 women in full-term pregnancies (11). Fetal and maternal mortality from pheochromocytoma is relatively high, reaching 26% and 17%, respectively (12), but this number greatly increases if left undiagnosed. With proper antepartum diagnosis, the rates fall from 17% to 0% for maternal mortality, and fetal losses fall from 26% to 15% (11). Insight into the rapid onset of PPCM in the presence of pheochromocytoma would enhance our knowledge of the importance of neurohormone disturbances for development of dilated cardiomyopathies and the pathophysiology of PPCM in general.

To the best of our knowledge, the increased rate of development of cardiomyopathy in gravid females with pheochromocytomas has not been studied in detail. We wonder whether pregnancy increases sensitivity to high catecholamine concentrations produced by the pheochromocytoma cells, or to an array of factors secreted by pheochromocytomas. Some arguments are in favor of a direct result of increased levels of catecholamines, experienced during pregnancy (13, 14). Cardiovascular morbidities that follow elevated catecholamine levels, e.g. from chronic cocaine abuse, become more pronounced during pregnancy (15, 16). Several observations have been made relating the myocardial damage found in patients

diagnosed with pheochromocytomas to that of patients treated with norepinephrine (NE) (17, 18). A further resemblance of the two diseases involves the cardiac functional improvement seen in patients whose pheochromocytoma has been excised and those in which catecholamine levels have been reduced to normal. Since it is believed that the major myocardial damage induced by the pheochromocytoma occurs from excessive release of catecholamines, an association can be drawn about the mode of damage induced by catecholamine overload. Studies involving catecholamine-induced cardiomyopathy have demonstrated that an excess of catecholamines down-regulated β-receptors while causing severe damage to myofibrils resulting in a global reduction of myocardial pump function. Cardiomyocytes incubated with increasing concentrations of NE exhibit increased cell death from hyper-contraction (19). It has also been posited that the oxidized products of catecholamines may be toxic, causing further cell damage (20). The effects of increased catecholamine secretion by pheochromocytoma cells might add up to elevated catecholamine levels with the stresses inherent in pregnancy (21).

To examine if changes in myocardial function arise solely from the release of catecholamines by pheochromocytoma cells or a complex of pheochromocytoma-derived factors, rats will receive implants of agarose spheres loaded with MPC cells. Non-gravid and gravid mice will be compared to determine the influence of pregnancy on pheochromocytoma-induced cardiomyopathy. The factors introduced during pregnancy such as increased female reproductive hormones, increased volume, and the presence of a fetus may act in concert with the pheochromocytoma to increase the effects of catecholamines. There exist a variety of hormones whose concentrations

greatly increase throughout pregnancy, significantly altering cardiovascular function. To determine which factors in the gravid state increase the heart's sensitivity to pheochromocytoma, we will initially concentrate on known gravid factors that amend cardiovascular function in conjunction with non-gravid rats with implanted pheochromocytoma cells.

6.2 Method

6.2.1 Cell Culture and Encapsulation

Rat pheochromocytoma cells (PC12, ATCC, VA) were maintained in F12K media (ATCC) with 10% heat-inactivated horse serum (Hyclone, Logan, UT), 5% FBS (Hyclone) and 100 units/ml penicillin/streptomyocin (Invitrogen, CA). Cells were grown at 37°C, 5% CO_2, and subcultured every 2 days. Agarose microspheres were developed as previously described (76). PC12 cells were scraped, centrifuged, and re-suspended in a preheated solution of 2.5% (w/w) agarose (Sigma-Aldrich, Type VII, St. Louis, MO) in 0.9% NaCl. The mixture was drawn into an Eppendorf Repeater Pipette with a 0.5 mL Combitip (VWR, MO) and 10 μL aliquots sheared into a mineral oil bath (~600 mL). The beads were separated using a 1,000 μm pore size nylon mesh (Small Parts, FL) and washed with PBS.

6.2.2 Animal Experiments

Female Black-6 mice (7-8 weeks old, 15-20 g) were obtained from Taconic. All animal studies were performed in accordance with protocols approved by the MIT Institutional Animal Care and Use Committee (IACUC), IACUC of Harvard Medical School, and the Guide for the Care and Use of Laboratory Animals published by the U.S. National Institutes of Health (NIH Publication No. 85-23, revised 1996). Osmotic pumps (Model 1004, CA) or agarose-encapsulated PC12 cells were implanted in the retro-peritoneal cavity adjacent to the kidneys to mimic the spatial release of pheochromocytoma cells. A total of 20 PC12 encapsulated agarose beads were

implanted into the retro-peritoneal space for an overall secretion rate of 9.2 ng of NE/day. The NE secretion rate was matched via osmotic pumps (Alzet) delivering 0.11 μL/hr loaded with 21 μM solution of NE in acidic saline (0.1 mg/mL ascorbic acid in saline).

Following implantation, mice were allowed to recover for a period of 7 days. On the 7^{th} day female mice were segregated into groups and those designated for the gravid state were separate into cages with a single male mouse of the same age. The female mice were visually inspected for plugs; if found, the male and female mice were separated. Those mice for which plugs were not found were monitored for the remainder of the study and the male mice were separated when the female was visibly gravid.

Catecholamine levels present in rats and mice were tracked through weekly blood draws via the retro-orbital plexus. The plasma catecholamine concentration was quantified by ELISA (Rocky Mountain Diagnostics). Control animals received osmotic pumps loaded with the ascorbic acid/saline carrier solution. Animals implanted with empty agarose beads and non-surgical, non-implanted animals had statistically identical cardiac dimensions and mRNA levels.

6.2.3 Echocardiographic Measurements

Transthoracic echocardiography was performed in anesthetized mice (2% isoflurane) using a 12-MHz probe and a Sonos 5500 ultrasonograph (Hewlett-Packard, MA). Left ventricular parameters and heart rates were obtained from M-mode interrogation in a short-axis view averaged from three separate cardiac cycles. Heart rates were greater than 400 beats per minute. The echocardiographer was blinded to mice genotypes. Cardiac contractile function was represented by the parameter LV fractional shortening (percentage), calculated as [(LV diastolic diameter - LV systolic diameter)/LV diastolic diameter] x 100.

6.2.4 Cardiomyocyte Protein Analysis

Hearts were excised, washed in PBS, and the LV separated and frozen in liquid nitrogen. Sections (2x2x2 mm) were weighed and sectioned in a microtome and lysed in 1 mL solution (20 mM Tris, 150 mM NaCl, NaOH pH 8.0, pH with NaOH, 1% Triton X-100, 0.1% SDS, 2 mM sodium orthovanadate, 2 mM PMSF, 50 mM NaF, protease inhibitor cocktail, Roche). Samples were boiled for 5 minutes with Laemmli sample buffer and separated on Nupage gels (Invitrogen). Cardiomyocytes incubated in growth media without PC12-conditioned media or norepinephrine served as controls. Proteins were transferred onto membranes using iBlot stacks (Invitrogen), blocked, and incubated with b-MHC (Abcam), periostin (Abcam), troponin I polyclonal (Abcam) antibody. Membranes were incubated with a goat anti-mouse monoclonal antibody (Santa Cruz Biotechnology, CA) at a 1:1,000 dilution for 2 hours at room temperature. The membranes were then washed in PBS-T (PBS with 0.05% Tween 20) and

incubated with the Western Supersignal Femto kit (Pierce, IL). The membranes were exposed on a FluorChem SP (Alpha Innotech, CA).

6.2.5 Histological Analyses

Animals were euthanized the hearts excised, rinsed in PBS, blotted dry, weighed, and pressure perfused (100 mmHg) with PBS for 5 minutes followed by 10% neutral buffered formalin (NBF) until visibly firm and pale. The hearts were placed in 10% NBF for 18h, processed, fixed in paraffin (Polysciences Inc., PA), and serial coronal sections were cut and stained with hematoxylin and eosin (Sigma-Aldrich) and Gomori's Trichrome (American HistoLabs Inc., MD). A pathologist, blinded to the treatment groups, graded the tissues. TUNEL assay was performed with an apoptosis kit (Millipore, MA) according to the manufacturer's instructions. Four to six images per heart were acquired on Leica microscope. Results were expressed as the number of apoptotic nuclei per total nuclei per image field.

6.2.6 Statistical Analysis

Results are presented as mean ± SD. Comparisons of data from two groups used Student's t test and for multiple groups, one-way ANOVA, or two-way ANOVA for repeated measurements (Minitab, PA). Contractility data and LV mRNA data were analyzed for statistical significance using two-way ANOVA followed by a TUKEY post-hoc test to determine significance. A value of $p < 0.05$ was considered statistically significant.

6.3 Results

6.3.1 Cardiac Morphology and Function

Cardiac dilation was more pronounced in Gravid Pheo mice ($p<0.01$ vs. control, $p<0.01$ vs. NE) compared to Pheo, NE, Gravid Controls and Control mice. Gravid Pheo mice developed an 8% greater degree of dilation over pheo mice ($p<0.01$) and 6% greater than gravid controls ($p<0.01$) (Table 6). These changes occurred despite the absence of significant increases in the SBP or heart rates over non-gravid mice, and both were statistically indistinguishable from Pheo and NE mice (Figure 20). Histologic analyses of cardiac tissue showed little microscopic difference between pheo, NE, and control animals (Figure 22). Of note, the gravid state had no effect on the fractional shortening as both Gravid Pheo and Pheo mice exhibited statistically identical fractional shortening (Figure 21). It must be noted that the gravid state itself affects cardiac dimensions, evident by the significantly increased LVEDD and LVESD and the decreased fractional shortening.

Table 6. Cardiac Morphology and Function for Gravid and Non-Gravid Mice.

Characteristic	Non-Gravid Control	Gravid Control	Non-Gravid NE	Non-Gravid Pheo	Gravid Pheo
No. Mice	4	5	5	6	5
Age (weeks)	7±2	7±2	7±2	7±2	7±2
LVWT (mm)	0.68±0.04	0.74±0.05	0.63±0.04	0.65±0.03	0.57±0.04
LVEDD (mm)	3.29±0.39	3.92±0.38	3.52±0.12	3.86±0.10 **,##	4.17±0.49
LVESD (mm)	1.76±0.35	2.50±0.17	2.32±0.28	2.85±0.22**,##	3.10±0.52
FS, %	46±5	35±4	34±7	25±5**,##	25±4

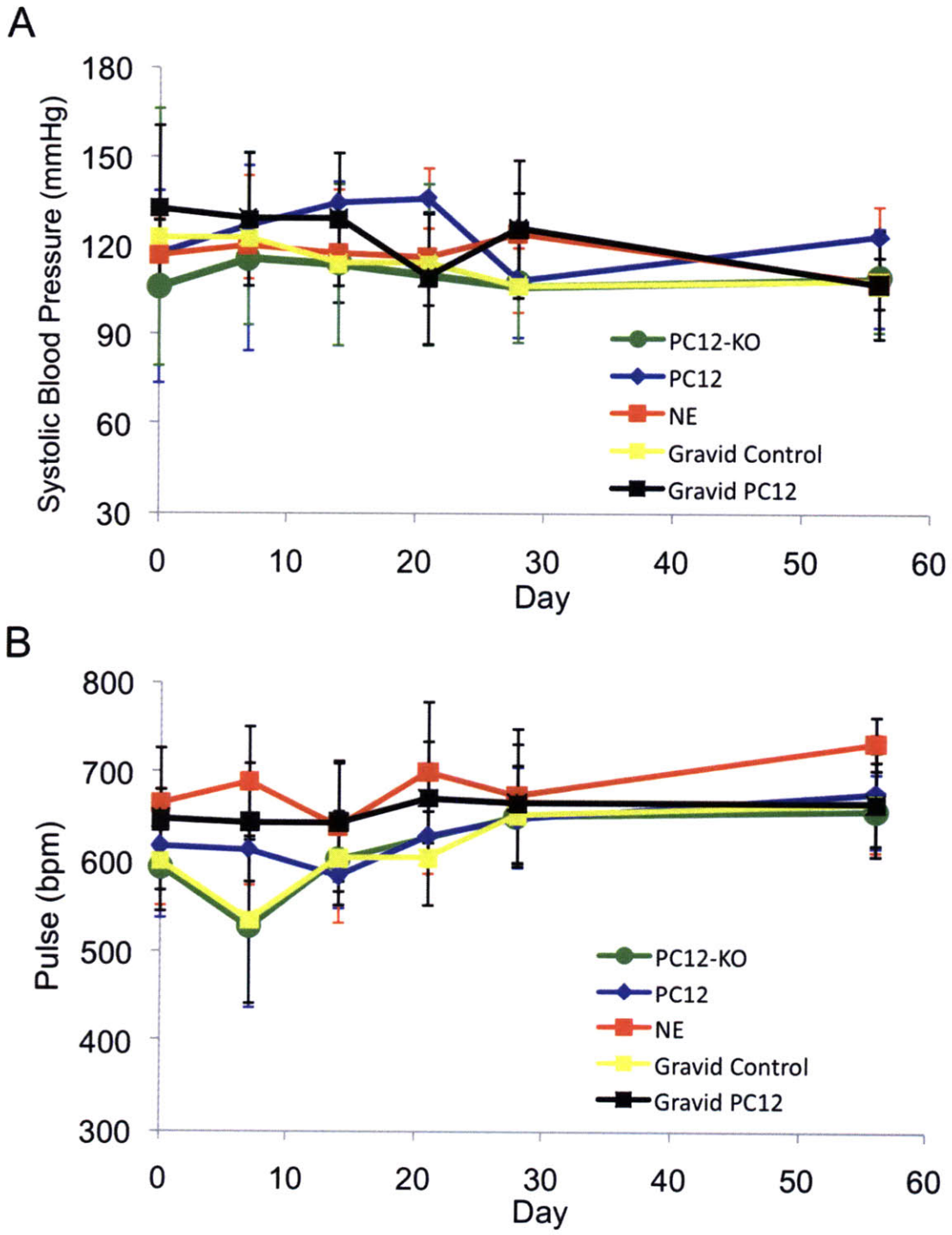

Figure 20. The gravid state induces no changes in hemodynamic state. Systolic Blood Pressure (A) and Pulse (B) remain unchanged in gravid mice compared to non-gravid counterparts. (n=4 animals per group).

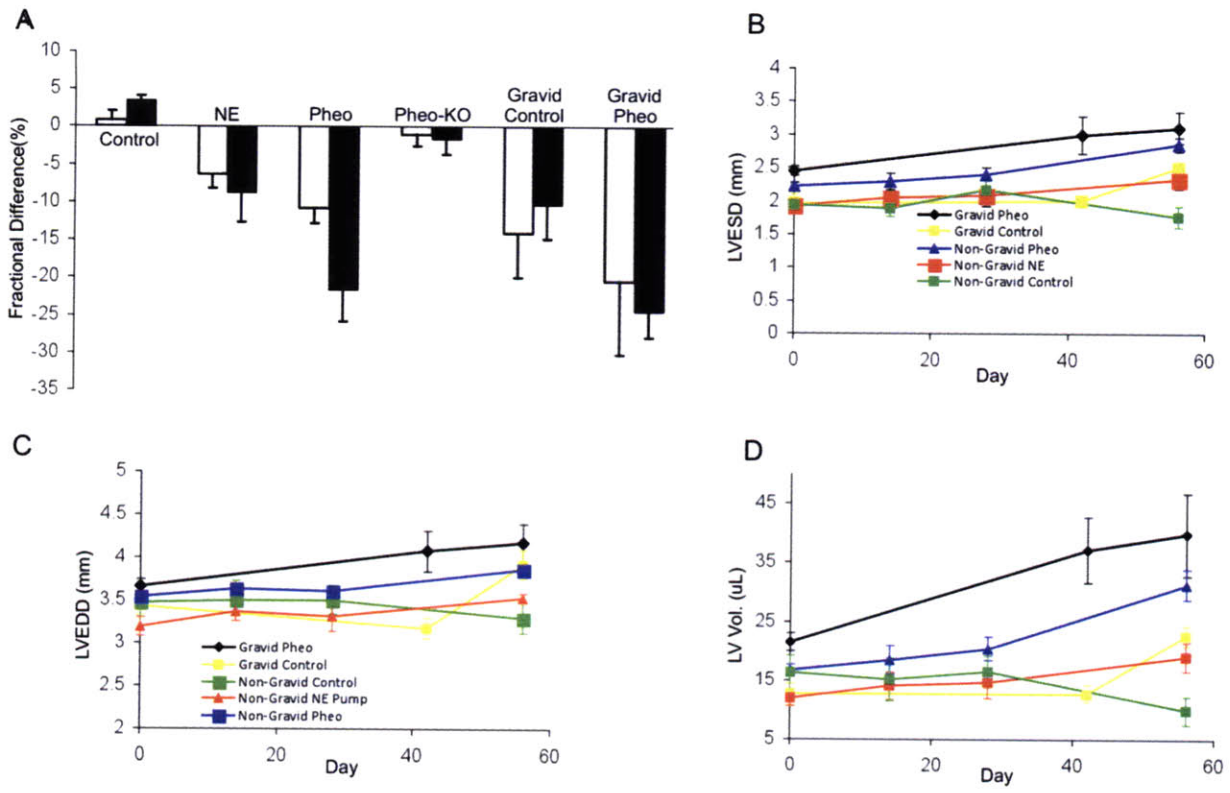

Figure 21. The gravid state increases the rate of cardiomyopathy development. (A) Change in fractional shortening (white) and ejection fraction (black) from Day 0 to Day 56 for Control, NE, Pheo, Pheo-KO, gravid control and gravid pheo mice. Pheochromocytoma-bearing gravid mice undergo an increased rate of increase of left ventricular end systolic (B) and diastolic (C) diameters. (D) LV volume increased at a greater rate in pheochromocytoma bearing gravid mice in comparison top their non-gravid counterparts.

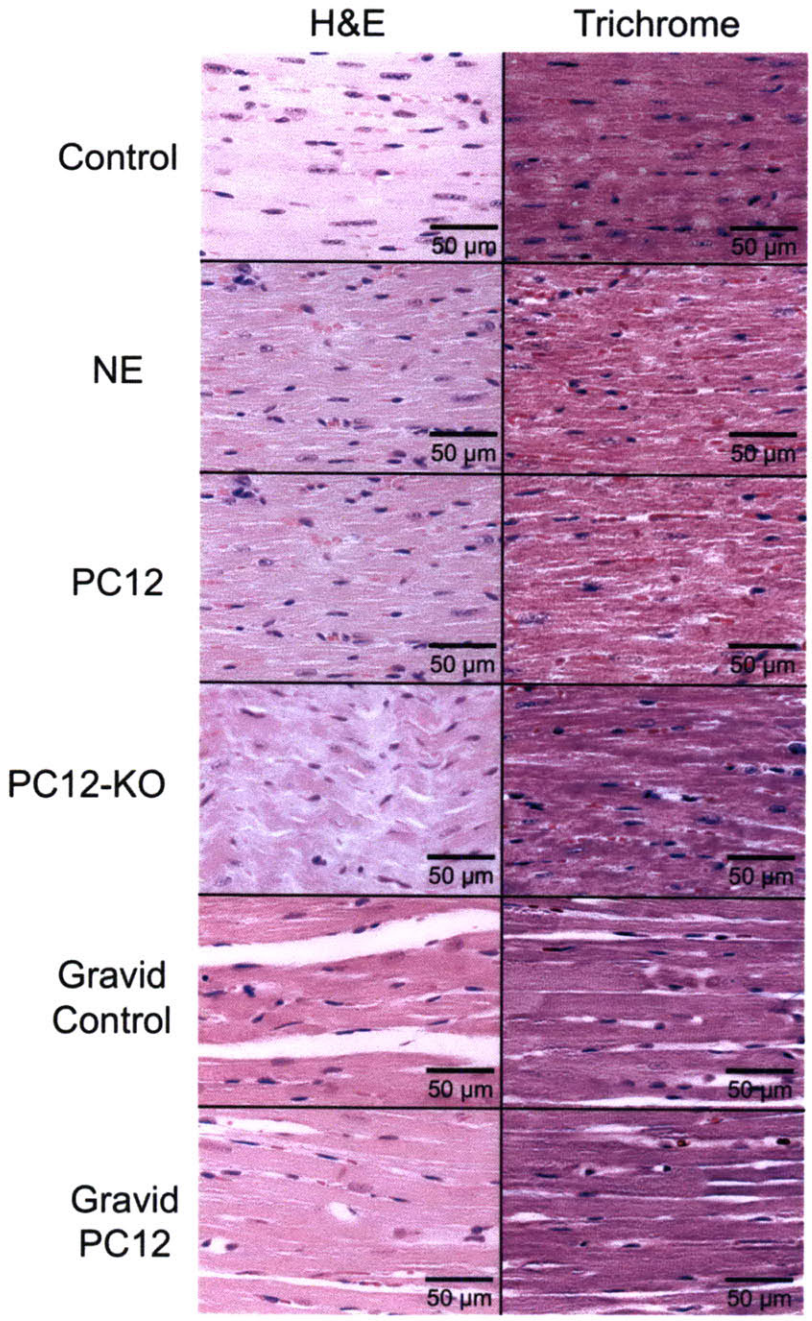

Figure 22. Low doses of NE released by pheochromocytoma cells and NE pumps in the gravid and non-gravid no results in histological damage. Representative images from the hearts of rats and mice stained with Hematoxylin and Eosin and Gomori's Trichrome. Histopathology of NE, Pheo ,Pheo-KO, Non-gravid Controls, and Gravid Pheo mice exhibited no myocyte disarray or fibrosis. All images taken at 40x magnification. (n=5 animals per group, n= 4 control animals per group).

6.3.2 Cardiac Protein Levels

Transcription of b-myosin heavy chain (β-MHC), a marker of the fetal gene program induced in hypertrophy, was increased by 20±6% % ($p<0.01$) in Pheo mice compared to control mice and by 18±7% ($p<0.01$) in gravid Pheo mice compared to gravid controls (Figure 19, A). The periostin gene is highly expressed in human heart failure models (110) and leads to cardiac dysfunction when up-regulated in rats (111). In line with these observations, periostin protein levels were up-regulated to a greater degree in pheo rats (200±60% greater than control, $p<0.05$), but were indistinguishable between gravid pheochromocytoma and control rats (7±5% gravid pheo over gravid control, $p>0.05$) (Figure 23, A).

Monocyte chemoattractant protein-1 (MCP-1), a C-C chemokine, is an inflammatory chemokine that activates leukocyte chemotaxis into inflamed or damaged tissue. MCP-1 is known to make a major contribution to the pathogenic role of inflammation in cardiovascular diseases. Recent studies have shown that levels of MCP-1 track with varying degrees of heart failure(112-114). Circulating MCP-1 levels were measured at 56 days post-implantation to asses cardiomyocyte health. Gravid Pheo mice exhibited 59±20% greater MCP-1 levels versus controls than their gravid control counter parts (Figure 23,B).

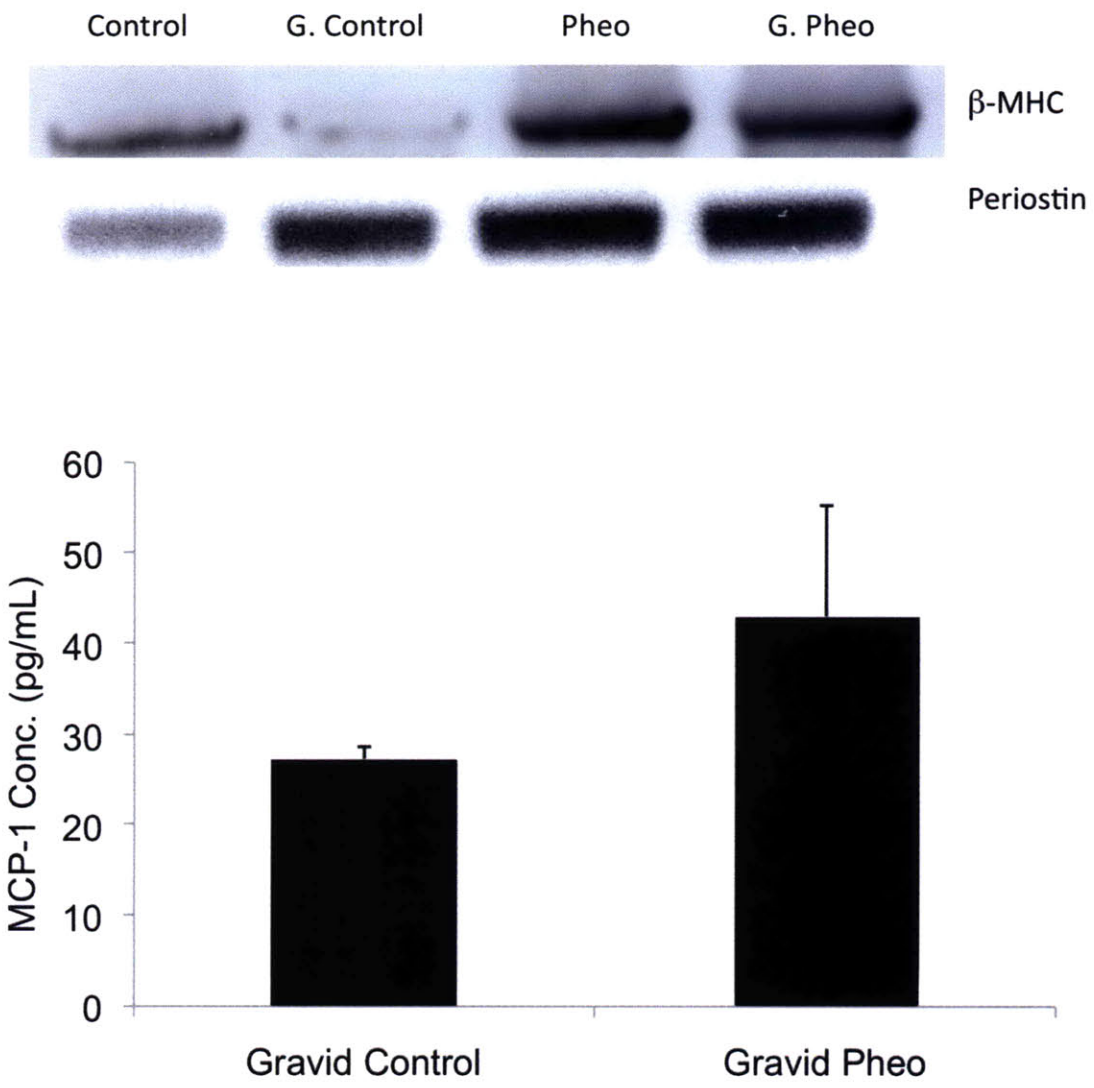

Figure 23. Implanted pheochromocytoma cells upregulate markers of cardiomyocyte remodeling. (A) Fetal gene markers of cardiomyocte remodeling, β myosin heavy chain (β-MHC) and periostin are upregulated in non-gravid and gravid pheochromocytoma bearing mice. (B) Monocyte chemotactic protein-1 plasma levels are upregulated in pheochromocytoma bearing gravid mice in comparison to gravid controls. G Pheo = Gravid Pheo and G Control = Gravid Control.

6.4 Discussion

Clinical observations indicate that gravid females with pheochromocytomas develop cardiomyopathy at an increased rate compared to non-gravid females. The ability of pheochromocytomas to induce cardiomyopathy has been well established but the exacerbation of cardiac pathology during the gravid state appears to be quite severe. Without proper diagnosis, fetal and maternal mortality reaches 26% and 17%, respectively(12). In addition to the effects of pheochromocytomas, the gravid state induces cardiac effects in its own right. Increased hemodynamic load and circulating gestational hormones, occurring during pregnancy and labor, may promote the development of hypertrophic cardiomyopathy. It therefore becomes pertinent to understand the events and factors contributing to the increased rate and severity of cardiomyopathy development in gravid females. The effects of pregnancy are evident in the gravid control mice, which experienced increased cardiac volume and diameter with decreased fractional shortening. These effects are most likely a result of the increased hemodynamic load and, to a lesser degree, the up-regulation of gestational hormones and the presence of a fetus. The implantation of pheochromocytoma cells exacerbates these symptoms more than the gravid control and non-gravid rats implanted with pheochromocytoma cells.

Pathological cardiomyopathy is associated with a well-documented pattern of gene expression, including reactivation of the fetal β-myosin heavy chain (β-MHC) and periostin. Such transcriptional profiles are utilized as measures of cardiomyopathy *in*

vivo and *in vitro*. Myocardial gene expression levels were increased to a greater degree in pheochromocytoma-bearing mice in the gravid and non-gravid state above controls. Increased expression of periostin and β-MHC, indicate greater cardiac remodeling, as experienced in previous studies of pheochromocytoma-bearing rats.

The results of this study indicate that the rate of development of pheochromocytoma-induced cardiomyopathy is increased during the gravid state. It may be that the increased cardiac stress inherent during pregnancy increases the heart's susceptibility to the effects of pheochromocytoma secretory factors, or alternatively it may be that these factors act in conjunction with pregnancy-related factors to induce a more severe cardiotoxic effect. Though the data are compelling, further experiments must be carried out to corroborate these initial studies. To properly compare the degree of cardiomyopathy, cardiac dimensions for each mouse must be compared to identical time points. The current study compares the degree of dilation and fractional shortening changes at day 42 and 56 for gravid animals to day 28 and 56 for non-gravid animals. These differences result from the inherent difficulties associated with gravid animal experiments, including the inability to control copulation date and temporal gravid-induced cardiomyopathy that precludes cardiac dimensional analysis during, and 7 days post, pregnancy. These limitations reflect the difficulty in working with gravid animals with a restricted time period.

7 Conclusions and Future Directions

The doctrine of *specific etiology* states that a specific factor causes disease and that a therapy can be designed to treat the disease by treating the single factor. Although this doctrine has helped us understand and control diseases, it does not explain the pathogenesis of complex processes. For example, heparan sulfate proteoglycan (HSPG) regulates vascular repair. Endothelial cells deficient in HSPGs have little to no effect on healing, yet the proteoglycan only accounts for a portion of the full effect (115). The non-proteoglycan component of endothelial cells has no effect alone, but determines and ensures the full effect when added to HSPG. This thesis utilizes a cardiomyopathy model to examine whether concepts developed for local factors and paracrine control extend to the systemic domain and endocrinologic regulation.

Pheochromocytomas and resulting cardiomyopathy are extremely relevant models for examining *specific pathogenesis* and are important in analyzing multifactorial-induced disease as a whole. The induction of cardiomyopathy by pheochromocytomas was previously attributed to the hypersecretion of catecholamines. The diagnosis of pheochromocytomas is frequently based on the physical manifestations of high levels of circulating catecholamines, a direct result of an advanced tumor. Animal models infused with similarly elevated catecholamine doses display the hallmark signs of cardiomyopathy including cardiac tissue necrosis, increased heart weight, and decreased heart function, leading to the prevailing theory that pheochromocytoma-induced cardiomyopathy results from catecholamine overload.

This thesis presents a body of work examining the mechanism of pheochromocytoma-induced cardiomyopathy. We developed a novel polymeric encapsulation system allowing for the implantation of pheochromocytoma cells in non-immune compromised animals to monitor the development of cardiomyopathy. We utilized agarose-encapulsated PC12 cells to demonstrate that pheochromocytoma-conditioned media induces cardiomyocytes to contract at a greater frequency than cardiomyocytes incubated with equivalent doses of norepinephrine. We further demonstrated that pheochromocytoma-conditioned media induces greater cardiomyocyte cytoskeletal remodeling than equivalent doses of norepinephrine.

The *in vivo* results mirrored our *in vitro* findings. We found that pheochromocytoma cells implanted in rats and mice induced a greater degree of cardiomyopathy than norepinephrine alone. The pheochromocytoma-bearing animals experienced a greater loss of cardiac function and a greater up-regulation of protein markers of cardiac remodeling compared to catecholamine-infused animals. Finally, we examined the role of pregnancy in our disease model and its ability to exacerbate pheochromocytoma-induced cardiomyopathy. Gravid pheochromocytoma-bearing mice experienced a more rapid loss of cardiac function and increased expansion of cardiac volume compared to non-gravid pheochromocytoma-bearing mice. Although the gravid state does not appear to increase the degree of cardiomyopathy induced by pheochromocytomas, the mice developed cardiac dilation and loss of function at a faster rate. It is therefore plausible that the gravid state increases the rate of cardiomyopathy development resulting in earlier physical signs and presentation of these tumors.

Future studies are necessary to examine the ability of pregnancy to increase the rate of cardiomyopathy development. To obtain an accurate estimate of cardiac function and morphology, echocardiograms must be taken prior to pregnancy and after one post-birth, the time required for the cardiac effects of pregnancy to abate. To properly compare cardiac function between gravid and non-gravid groups it will be necessary to match time points at which echocardiograms are taken of the gravid and non-gravid mice. This requires a more efficient way of inducing mating earlier in the experiment. The studies described in this thesis involved segregating male and female mice into separate cages seven days following implantation. Mating occurred anywhere in between the date of segregation to ten days post-segregation, requiring a later echocardiogram date at 42-days post-implantation. Alternative methods or dates of implantation and segregation must be explored to decrease this time period.

8 References

1. Stenstrom, G., and Svardsudd, K. 1986. Pheochromocytoma in Sweden 1958-1981. An analysis of the National Cancer Registry Data. *Acta Med Scand* 220:225-232.
2. Pomares, F.J., Canas, R., Rodriguez, J.M., Hernandez, A.M., Parrilla, P., and Tebar, F.J. 1998. Differences between sporadic and multiple endocrine neoplasia type 2A phaeochromocytoma. *Clin Endocrinol (Oxf)* 48:195-200.
3. Inabnet, W.B., Caragliano, P., and Pertsemlidis, D. 2000. Pheochromocytoma: inherited associations, bilaterality, and cortex preservation. *Surgery* 128:1007-1011;discussion 1011-1002.
4. Bravo, E.L. 1991. Pheochromocytoma: new concepts and future trends. *Kidney Int* 40:544-556.
5. Karagiannis, A., Mikhailidis, D.P., Athyros, V.G., and Harsoulis, F. 2007. Pheochromocytoma: an update on genetics and management. *Endocr Relat Cancer* 14:935-956.
6. Baysal, B.E., Ferrell, R.E., Willett-Brozick, J.E., Lawrence, E.C., Myssiorek, D., Bosch, A., van der Mey, A., Taschner, P.E., Rubinstein, W.S., Myers, E.N., et al. 2000. Mutations in SDHD, a mitochondrial complex II gene, in hereditary paraganglioma. *Science* 287:848-851.
7. Niemann, S., and Muller, U. 2000. Mutations in SDHC cause autosomal dominant paraganglioma, type 3. *Nat Genet* 26:268-270.
8. Astuti, D., Latif, F., Dallol, A., Dahia, P.L., Douglas, F., George, E., Skoldberg, F., Husebye, E.S., Eng, C., and Maher, E.R. 2001. Gene mutations in the succinate dehydrogenase subunit SDHB cause susceptibility to familial pheochromocytoma and to familial paraganglioma. *Am J Hum Genet* 69:49-54.
9. Neumann, H.P., Bausch, B., McWhinney, S.R., Bender, B.U., Gimm, O., Franke, G., Schipper, J., Klisch, J., Altehoefer, C., Zerres, K., et al. 2002. Germ-line mutations in nonsyndromic pheochromocytoma. *N Engl J Med* 346:1459-1466.

10. Amar, L., Bertherat, J., Baudin, E., Ajzenberg, C., Bressac-de Paillerets, B., Chabre, O., Chamontin, B., Delemer, B., Giraud, S., Murat, A., et al. 2005. Genetic testing in pheochromocytoma or functional paraganglioma. *J Clin Oncol* 23:8812-8818.
11. John, H., Ziegler, W.H., Hauri, D., and Jaeger, P. 1999. Pheochromocytomas: can malignant potential be predicted? *Urology* 53:679-683.
12. Ross, E.J., Prichard, B.N., Kaufman, L., Robertson, A.I., and Harries, B.J. 1967. Preoperative and operative management of patients with phaeochromocytoma. *Br Med J* 1:191-198.
13. Perry, L.B., and Gould, A.B., Jr. 1972. The anesthetic management of pheochromocytoma effect of preoperative adrenergic blocking drugss. *Anesth Analg* 51:36-40.
14. Serfas, D., Shoback, D.M., and Lorell, B.H. 1983. Phaeochromocytoma and hypertrophic cardiomyopathy: apparent suppression of symptoms and noradrenaline secretion by calcium-channel blockade. *Lancet* 2:711-713.
15. Lenders, J.W., Sluiter, H.E., Thien, T., and Willemsen, J. 1985. Treatment of a phaeochromocytoma of the urinary bladder with nifedipine. *Br Med J (Clin Res Ed)* 290:1624-1625.
16. Lehmann, H.U., Hochrein, H., Witt, E., and Mies, H.W. 1983. Hemodynamic effects of calcium antagonists. Review. *Hypertension* 5:II66-73.
17. Warren, S., and Chute, R.N. 1972. Pheochromocytoma. *Cancer* 29:327-331.
18. Rosenbaum, J.S., Billingham, M.E., Ginsburg, R., Tsujimoto, G., Lurie, K.G., and Hoffman, B.B. 1988. Cardiomyopathy in a rat model of pheochromocytoma. Morphological and functional alterations. *Am J Cardiovasc Pathol* 1:389-399.
19. Ohta, S., Lai, E.W., Taniguchi, S., Tischler, A.S., Alesci, S., and Pacak, K. 2006. Animal models of pheochromocytoma including NIH initial experience. *Ann N Y Acad Sci* 1073:300-305.
20. Tischler, A.S., Powers, J.F., and Alroy, J. 2004. Animal models of pheochromocytoma. *Histol Histopathol* 19:883-895.
21. Tsujimoto, G., Hashimoto, K., and Hoffman, B.B. 1985. Effects of pheochromocytoma on cardiovascular alpha adrenergic receptor system. *Heart Vessels* 1:152-157.

22. Tsujimoto, G., Manger, W.M., and Hoffman, B.B. 1984. Desensitization of beta-adrenergic receptors by pheochromocytoma. *Endocrinology* 114:1272-1278.

23. Snavely, M.D., Motulsky, H.J., O'Connor, D.T., Ziegler, M.G., and Insel, P.A. 1982. Adrenergic receptors in human and experimental pheochromocytoma. *Clin Exp Hypertens A* 4:829-848.

24. Fedak, P.W., Altamentova, S.M., Weisel, R.D., Nili, N., Ohno, N., Verma, S., Lee, T.Y., Kiani, C., Mickle, D.A., Strauss, B.H., et al. 2003. Matrix remodeling in experimental and human heart failure: a possible regulatory role for TIMP-3. *Am J Physiol Heart Circ Physiol* 284:H626-634.

25. Tischler, A.S. 2002. Chromaffin cells as models of endocrine cells and neurons. *Ann N Y Acad Sci* 971:366-370.

26. Rosenbaum, J.S., Ginsburg, R., Billingham, M.E., and Hoffman, B.B. 1987. Effects of adrenergic receptor antagonists on cardiac morphological and functional alterations in rats harboring pheochromocytoma. *J Pharmacol Exp Ther* 241:354-360.

27. Chappel, C.I., Rona, G., Balazs, T., and Gaudry, R. 1959. Comparison of cardiotoxic actions of certain sympathomimetic amines. *Can J Biochem Physiol* 37:35-42.

28. Blaiklock, R.G., Hirsh, E.M., Dapson, S., Paino, B., and Lehr, D. 1981. Epinephrine induced myocardial necrosis: effects of aminophylline and adrenergic blockade. *Res Commun Chem Pathol Pharmacol* 34:179-192.

29. Downing, S.E., and Lee, J.C. 1983. Contribution of alpha-adrenoceptor activation to the pathogenesis of norepinephrine cardiomyopathy. *Circ Res* 52:471-478.

30. Mehes, G., Papp, G., and Rajkovits, K. 1967. Effect of adrenergic alpha- and beta-receptor blocking drugs on the myocardial lesions induced by sympathomimetic amines. *Acta Physiol Acad Sci Hung* 32:175-184.

31. Smith-Hicks, C.L., Sizer, K.C., Powers, J.F., Tischler, A.S., and Costantini, F. 2000. C-cell hyperplasia, pheochromocytoma and sympathoadrenal malformation in a mouse model of multiple endocrine neoplasia type 2B. *Embo J* 19:612-622.

32. Podsypanina, K., Lee, R.T., Politis, C., Hennessy, I., Crane, A., Puc, J., Neshat, M., Wang, H., Yang, L., Gibbons, J., et al. 2001. An inhibitor of mTOR reduces

neoplasia and normalizes p70/S6 kinase activity in Pten+/- mice. *Proc Natl Acad Sci U S A* 98:10320-10325.

33. You, M.J., Castrillon, D.H., Bastian, B.C., O'Hagan, R.C., Bosenberg, M.W., Parsons, R., Chin, L., and DePinho, R.A. 2002. Genetic analysis of Pten and Ink4a/Arf interactions in the suppression of tumorigenesis in mice. *Proc Natl Acad Sci U S A* 99:1455-1460.
34. Hoffman, B.B. 1991. Adrenergic pharmacology in rats harboring pheochromocytoma. *Hypertension* 18:III35-39.
35. Lehmann, M.H., Kuhnert, H., Muller, S., and Sigusch, H.H. 1998. Monocyte chemoattractant protein 1 (MCP-1) gene expression in dilated cardiomyopathy. *Cytokine* 10:739-746.
36. Szakacs, J.E., and Cannon, A. 1958. L-Norepinephrine myocarditis. *Am J Clin Pathol* 30:425-434.
37. Mann, D.L., Kent, R.L., Parsons, B., and Cooper, G.t. 1992. Adrenergic effects on the biology of the adult mammalian cardiocyte. *Circulation* 85:790-804.
38. Kline, I.K. 1961. Myocardial alterations associated with pheochromocytomas. *Am J Pathol* 38:539-551.
39. Sardesai, S.H., Mourant, A.J., Sivathandon, Y., Farrow, R., and Gibbons, D.O. 1990. Phaeochromocytoma and catecholamine induced cardiomyopathy presenting as heart failure. *Br Heart J* 63:234-237.
40. Jiang, J.P., and Downing, S.E. 1990. Catecholamine cardiomyopathy: review and analysis of pathogenetic mechanisms. *Yale J Biol Med* 63:581-591.
41. Briest, W., Holzl, A., Rassler, B., Deten, A., Leicht, M., Baba, H.A., and Zimmer, H.G. 2001. Cardiac remodeling after long term norepinephrine treatment in rats. *Cardiovasc Res* 52:265-273.
42. Nanda, A.S., Feldman, A., and Liang, C.S. 1995. Acute reversal of pheochromocytoma-induced catecholamine cardiomyopathy. *Clin Cardiol* 18:421-423.
43. Yankopoulos, N.A., Montero, A.C., Curd, W.G., Jr., Kahil, M.E., and Condon, R.E. 1974. Observations on myocardial function during chronic catecholamine oversecretion. *Chest* 66:585-587.

44. Frustaci, A., Loperfido, F., Gentiloni, N., Caldarulo, M., Morgante, E., and Russo, M.A. 1991. Catecholamine-induced cardiomyopathy in multiple endocrine neoplasia. A histologic, ultrastructural, and biochemical study. *Chest* 99:382-385.

45. Imperadore, F., Azzolini, M., Piscioli, F., Pusiol, T., Capitanio, A., and Vergara, G. 2002. A rare cause of cardiogenic shock: catecholamine cardiomyopathy of pheochromocytoma. *Ital Heart J* 3:375-378.

46. Yoshida, K., Sasaguri, M., Kinoshita, A., Ideishi, M., Ikeda, M., and Arakawa, K. 1990. A case of a clinically "silent" pheochromocytoma. *Jpn J Med* 29:27-31.

47. Greene, L.A., and Tischler, A.S. 1976. Establishment of a noradrenergic clonal line of rat adrenal pheochromocytoma cells which respond to nerve growth factor. *Proc Natl Acad Sci U S A* 73:2424-2428.

48. Powers, J.F., Evinger, M.J., Tsokas, P., Bedri, S., Alroy, J., Shahsavari, M., and Tischler, A.S. 2000. Pheochromocytoma cell lines from heterozygous neurofibromatosis knockout mice. *Cell Tissue Res* 302:309-320.

49. Dixon, D.N., Loxley, R.A., Barron, A., Cleary, S., and Phillips, J.K. 2005. Comparative studies of PC12 and mouse pheochromocytoma-derived rodent cell lines as models for the study of neuroendocrine systems. *In Vitro Cell Dev Biol Anim* 41:197-206.

50. Brown, C.S., and Bertolet, B.D. 1998. Peripartum cardiomyopathy: a comprehensive review. *Am J Obstet Gynecol* 178:409-414.

51. Bhakta, P., Biswas, B.K., and Banerjee, B. 2007. Peripartum cardiomyopathy: review of the literature. *Yonsei Med J* 48:731-747.

52. Homans, D.C. 1985. Peripartum cardiomyopathy. *N Engl J Med* 312:1432-1437.

53. Pearson, G.D., Veille, J.C., Rahimtoola, S., Hsia, J., Oakley, C.M., Hosenpud, J.D., Ansari, A., and Baughman, K.L. 2000. Peripartum cardiomyopathy: National Heart, Lung, and Blood Institute and Office of Rare Diseases (National Institutes of Health) workshop recommendations and review. *Jama* 283:1183-1188.

54. Ansari, A.A., Fett, J.D., Carraway, R.E., Mayne, A.E., Onlamoon, N., and Sundstrom, J.B. 2002. Autoimmune mechanisms as the basis for human peripartum cardiomyopathy. *Clin Rev Allergy Immunol* 23:301-324.

55. Kemp, V.H., and Hatmaker, D.D. 1989. Stress and social support in high-risk pregnancy. *Res Nurs Health* 12:331-336.

56. Suzuki, A., Hashino, M., Chiba, H., Saito, H., Notake, Y., Yanaihara, T., and Nakayama, T. 1989. [Correlation between the levels of catecholamines (noradrenaline, adrenaline) and adrenal steroids (DHA-S, cortisol) in maternal and fetal blood during pregnancy and labor]. *Nippon Naibunpi Gakkai Zasshi* 65:704-714.

57. Tidswell, M. 2004. Peripartum cardiomyopathy. *Crit Care Clin* 20:777-788, xi.

58. Hilfiker-Kleiner, D., Kaminski, K., Podewski, E., Bonda, T., Schaefer, A., Sliwa, K., Forster, O., Quint, A., Landmesser, U., Doerries, C., et al. 2007. A cathepsin D-cleaved 16 kDa form of prolactin mediates postpartum cardiomyopathy. *Cell* 128:589-600.

59. Hayakawa, Y., Chandra, M., Miao, W., Shirani, J., Brown, J.H., Dorn, G.W., 2nd, Armstrong, R.C., and Kitsis, R.N. 2003. Inhibition of cardiac myocyte apoptosis improves cardiac function and abolishes mortality in the peripartum cardiomyopathy of Galpha(q) transgenic mice. *Circulation* 108:3036-3041.

60. Wilkenfeld, C., Cohen, M., Lansman, S.L., Courtney, M., Dische, M.R., Pertsemlidis, D., and Krakoff, L.R. 1992. Heart transplantation for end-stage cardiomyopathy caused by an occult pheochromocytoma. *J Heart Lung Transplant* 11:363-366.

61. Bravo, E.L., and Tagle, R. 2003. Pheochromocytoma: state-of-the-art and future prospects. *Endocr Rev* 24:539-553.

62. Meijer, W.G., Copray, S.C., Hollema, H., Kema, I.P., Zwart, N., Mantingh-Otter, I., Links, T.P., Willemse, P.H., and de Vries, E.G. 2003. Catecholamine-synthesizing enzymes in carcinoid tumors and pheochromocytomas. *Clin Chem* 49:586-593.

63. Reisch, N., Peczkowska, M., Januszewicz, A., and Neumann, H.P. 2006. Pheochromocytoma: presentation, diagnosis and treatment. *J Hypertens* 24:2331-2339.

64. Gifford, R.W., Jr., Bravo, E.L., and Manger, W.M. 1985. Diagnosis and management of pheochromocytoma. *Cardiology* 72 Suppl 1:126-130.

65. Lenders, J.W., Keiser, H.R., Goldstein, D.S., Willemsen, J.J., Friberg, P., Jacobs, M.C., Kloppenborg, P.W., Thien, T., and Eisenhofer, G. 1995. Plasma

metanephrines in the diagnosis of pheochromocytoma. *Ann Intern Med* 123:101-109.

66. Wiswell, J.G., and Crago, R.M. 1969. Reversible cardiomyopathy with pheochromocytoma. *Trans Am Clin Climatol Assoc* 80:185-195.
67. Farroni, J.A. 2005. Pheochromocytoma presenting as heart failure. *Prog Cardiovasc Nurs* 20:117-119.
68. Gatzoulis, K.A., Tolis, G., Theopistou, A., Gialafos, J.H., and Toutouzas, P.K. 1998. Cardiomyopathy due to a pheochromocytoma. A reversible entity. *Acta Cardiol* 53:227-229.
69. Schuiki, E.R., Jenni, R., Amann, F.W., and Ziegler, W.H. 1993. A reversible form of apical left ventricular hypertrophy associated with pheochromocytoma. *J Am Soc Echocardiogr* 6:327-331.
70. Wood, R., Commerford, P.J., Rose, A.G., and Tooke, A. 1991. Reversible catecholamine-induced cardiomyopathy. *Am Heart J* 121:610-613.
71. Yarmush, M.L., Dunn, J.C., and Tompkins, R.G. 1992. Assessment of artificial liver support technology. *Cell Transplant* 1:323-341.
72. Foy, B.D., Rotem, A., Toner, M., Tompkins, R.G., and Yarmush, M.L. 1994. A device to measure the oxygen uptake rate of attached cells: importance in bioartificial organ design. *Cell Transplant* 3:515-527.
73. Landry, J., Bernier, D., Ouellet, C., Goyette, R., and Marceau, N. 1985. Spheroidal aggregate culture of rat liver cells: histotypic reorganization, biomatrix deposition, and maintenance of functional activities. *J Cell Biol* 101:914-923.
74. Cheng, M., Park, H., Engelmayr, G.C., Moretti, M., and Freed, L.E. 2007. Effects of regulatory factors on engineered cardiac tissue in vitro. *Tissue Eng* 13:2709-2719.
75. Drubin, D.A., Garakani, A.M., and Silver, P.A. 2006. Motion as a phenotype: the use of live-cell imaging and machine visual screening to characterize transcription-dependent chromosome dynamics. *BMC Cell Biol* 7:19.
76. Khademhosseini, A., May, M.H., and Sefton, M.V. 2005. Conformal coating of mammalian cells immobilized onto magnetically driven beads. *Tissue Eng* 11:1797-1806.

77. Rozen, S., Skaletsky, H.J. . 2000. Primer3 on the WWW for general users and for biologist programmers. In *Bioinformatics Methods and Protocols: Methods in Molecular Biology*. S. Krawetz, Misener, S., editor. Totowa, NJ: Humana Press. 365-386.

78. Roberts, T., De Boni, U., and Sefton, M.V. 1996. Dopamine secretion by PC12 cells microencapsulated in a hydroxyethyl methacrylate--methyl methacrylate copolymer. *Biomaterials* 17:267-275.

79. Waldo, S.W., Beede, J., Isakson, S., Villard-Saussine, S., Fareh, J., Clopton, P., Fitzgerald, R.L., and Maisel, A.S. 2008. Pro-B-type natriuretic peptide levels in acute decompensated heart failure. *J Am Coll Cardiol* 51:1874-1882.

80. Hobbs, F.D., Davis, R.C., Roalfe, A.K., Hare, R., Davies, M.K., and Kenkre, J.E. 2002. Reliability of N-terminal pro-brain natriuretic peptide assay in diagnosis of heart failure: cohort study in representative and high risk community populations. *Bmj* 324:1498.

81. Taimor, G., Schluter, K.D., Frischkopf, K., Flesch, M., Rosenkranz, S., and Piper, H.M. 1999. Autocrine regulation of TGF beta expression in adult cardiomyocytes. *J Mol Cell Cardiol* 31:2127-2136.

82. Condorelli, G., Drusco, A., Stassi, G., Bellacosa, A., Roncarati, R., Iaccarino, G., Russo, M.A., Gu, Y., Dalton, N., Chung, C., et al. 2002. Akt induces enhanced myocardial contractility and cell size in vivo in transgenic mice. *Proc Natl Acad Sci U S A* 99:12333-12338.

83. Stromer, M.H. 1998. The cytoskeleton in skeletal, cardiac and smooth muscle cells. *Histol Histopathol* 13:283-291.

84. Towbin, J.A., Hejtmancik, J.F., Brink, P., Gelb, B., Zhu, X.M., Chamberlain, J.S., McCabe, E.R., and Swift, M. 1993. X-linked dilated cardiomyopathy. Molecular genetic evidence of linkage to the Duchenne muscular dystrophy (dystrophin) gene at the Xp21 locus. *Circulation* 87:1854-1865.

85. Li, D., Tapscoft, T., Gonzalez, O., Burch, P.E., Quinones, M.A., Zoghbi, W.A., Hill, R., Bachinski, L.L., Mann, D.L., and Roberts, R. 1999. Desmin mutation responsible for idiopathic dilated cardiomyopathy. *Circulation* 100:461-464.

86. Dalakas, M.C., Park, K.Y., Semino-Mora, C., Lee, H.S., Sivakumar, K., and Goldfarb, L.G. 2000. Desmin myopathy, a skeletal myopathy with

cardiomyopathy caused by mutations in the desmin gene. *N Engl J Med* 342:770-780.

87. Vasile, V.C., Ommen, S.R., Edwards, W.D., and Ackerman, M.J. 2006. A missense mutation in a ubiquitously expressed protein, vinculin, confers susceptibility to hypertrophic cardiomyopathy. *Biochem Biophys Res Commun* 345:998-1003.

88. Sato, H., Nagai, T., Kuppuswamy, D., Narishige, T., Koide, M., Menick, D.R., and Cooper, G.t. 1997. Microtubule stabilization in pressure overload cardiac hypertrophy. *J Cell Biol* 139:963-973.

89. Heling, A., Zimmermann, R., Kostin, S., Maeno, Y., Hein, S., Devaux, B., Bauer, E., Klovekorn, W.P., Schlepper, M., Schaper, W., et al. 2000. Increased expression of cytoskeletal, linkage, and extracellular proteins in failing human myocardium. *Circ Res* 86:846-853.

90. Kostin, S., Hein, S., Arnon, E., Scholz, D., and Schaper, J. 2000. The cytoskeleton and related proteins in the human failing heart. *Heart Fail Rev* 5:271-280.

91. Kohane, D.S., Tse, J.Y., Yeo, Y., Padera, R., Shubina, M., and Langer, R. 2006. Biodegradable polymeric microspheres and nanospheres for drug delivery in the peritoneum. *J Biomed Mater Res A* 77:351-361.

92. Rona, G. 1985. Catecholamine cardiotoxicity. *J Mol Cell Cardiol* 17:291-306.

93. Wheatley, A.M., Thandroyen, F.T., and Opie, L.H. 1985. Catecholamine-induced myocardial cell damage: catecholamines or adrenochrome. *J Mol Cell Cardiol* 17:349-359.

94. Downing, S.E., and Chen, V. 1985. Myocardial injury following endogenous catecholamine release in rabbits. *J Mol Cell Cardiol* 17:377-387.

95. Laycock, S.K., McMurray, J., Kane, K.A., and Parratt, J.R. 1995. Effects of chronic norepinephrine administration on cardiac function in rats. *J Cardiovasc Pharmacol* 26:584-589.

96. Communal, C., Singh, K., Pimentel, D.R., and Colucci, W.S. 1998. Norepinephrine stimulates apoptosis in adult rat ventricular myocytes by activation of the beta-adrenergic pathway. *Circulation* 98:1329-1334.

97. Simons, M., and Downing, S.E. 1985. Coronary vasoconstriction and catecholamine cardiomyopathy. *Am Heart J* 109:297-304.

98. Kahn, D.S., Rona, G., and Chappel, C.I. 1969. Isoproterenol-induced cardiac necrosis. *Ann N Y Acad Sci* 156:285-293.

99. Ferrans, V.J., Hibbs, R.G., Black, W.C., and Weilbaecher, D.G. 1964. Isoproterenol-Induced Myocardial Necrosis. a Histochemical and Electron Microscopic Study. *Am Heart J* 68:71-90.

100. Salomon, P., Przewlocka-Kosmala, M., and Orda, A. 2003. [Plasma levels of brain natriuretic peptide, cyclic 3'5'-guanosine monophosphate, endothelin 1, and noradrenaline in patients with chronic congestive heart failure]. *Pol Arch Med Wewn* 109:43-48.

101. Minguell, E. 2004. Clinical Use of Markers of Neurohormonal Activation in Heart Failure. *Revista Espanola de Cardiologia* 57:347-356.

102. Fedak, P.W., Smookler, D.S., Kassiri, Z., Ohno, N., Leco, K.J., Verma, S., Mickle, D.A., Watson, K.L., Hojilla, C.V., Cruz, W., et al. 2004. TIMP-3 deficiency leads to dilated cardiomyopathy. *Circulation* 110:2401-2409.

103. Swynghedauw, B. 1999. Molecular mechanisms of myocardial remodeling. *Physiol Rev* 79:215-262.

104. Favia, G., Lumachi, F., Polistina, F., and D'Amico, D.F. 1998. Pheochromocytoma, a rare cause of hypertension: long-term follow-up of 55 surgically treated patients. *World J Surg* 22:689-693; discussion 694.

105. Yamazaki, T., Lee, J.D., Shimizu, H., Uzui, H., and Ueda, T. 2004. Circulating matrix metalloproteinase-2 is elevated in patients with congestive heart failure. *Eur J Heart Fail* 6:41-45.

106. Taub, D.D., and Oppenheim, J.J. 1994. Chemokines, inflammation and the immune system. *Ther Immunol* 1:229-246.

107. Aukrust, P., Ueland, T., Muller, F., Andreassen, A.K., Nordoy, I., Aas, H., Kjekshus, J., Simonsen, S., Froland, S.S., and Gullestad, L. 1998. Elevated circulating levels of C-C chemokines in patients with congestive heart failure. *Circulation* 97:1136-1143.

108. Specht, H., Peterziel, H., Bajohrs, M., Gerdes, H.H., Krieglstein, K., and Unsicker, K. 2003. Transforming growth factor beta2 is released from PC12 cells via the regulated pathway of secretion. *Mol Cell Neurosci* 22:75-86.

109. Moller, J.C., Kruttgen, A., Burmester, R., Weis, J., Oertel, W.H., and Shooter, E.M. 2006. Release of interleukin-6 via the regulated secretory pathway in PC12 cells. *Neurosci Lett* 400:75-79.

110. Urasawa, K., Yoshida, I., Takagi, C., Onozuka, H., Mikami, T., Kawaguchi, H., and Kitabatake, A. 1996. Enhanced expression of beta-adrenergic receptor kinase 1 in the hearts of cardiomyopathic Syrian hamsters, BIO53.58. *Biochem Biophys Res Commun* 219:26-30.

111. Katsuragi, N., Morishita, R., Nakamura, N., Ochiai, T., Taniyama, Y., Hasegawa, Y., Kawashima, K., Kaneda, Y., Ogihara, T., and Sugimura, K. 2004. Periostin as a novel factor responsible for ventricular dilation. *Circulation* 110:1806-1813.

112. Frangogiannis, N.G., Smith, C.W., and Entman, M.L. 2002. The inflammatory response in myocardial infarction. *Cardiovasc Res* 53:31-47.

113. Frangogiannis, N.G., Perrard, J.L., Mendoza, L.H., Burns, A.R., Lindsey, M.L., Ballantyne, C.M., Michael, L.H., Smith, C.W., and Entman, M.L. 1998. Stem cell factor induction is associated with mast cell accumulation after canine myocardial ischemia and reperfusion. *Circulation* 98:687-698.

114. Nian, M., Lee, P., Khaper, N., and Liu, P. 2004. Inflammatory cytokines and postmyocardial infarction remodeling. *Circ Res* 94:1543-1553.

115. Nugent, M.A., Karnovsky, M.J., and Edelman, E.R. 1993. Vascular cell-derived heparan sulfate shows coupled inhibition of basic fibroblast growth factor binding and mitogenesis in vascular smooth muscle cells. *Circ Res* 73:1051-1060.